THE JOURNAL OF COMPARATIVE NEUROLOGY 375:552–582 (1996)

# Organization of Connections Between the Amygdaloid Complex and the Perirhinal and Parahippocampal Cortices in Macaque Monkeys

LISA STEFANACCI, WENDY A. SUZUKI, AND DAVID G. AMARAL
Group in Neurosciences, UCSD, La Jolla, California 92037 (L.S.); Laboratory of Neuropsychology, NIMH, NIH, Bethesda, Maryland 20892 (W.A.S.); Department of Psychiatry and Center for Neuroscience, UC Davis, Davis, California 95616 (D.G.A.)

ABSTRACT

Neuroanatomical studies in macaque monkeys have demonstrated that the perirhinal and parahippocampal (PRPH) cortices are strongly interconnected with the hippocampal formation. Recent behavioral evidence indicates that these cortical regions are importantly involved in normal recognition memory function. The PRPH cortices are also interconnected with the amygdaloid complex, although comparatively little is known about the precise topography of these connections. We investigated the topographic organization of reciprocal connections between the amygdala and the PRPH cortices by placing anterograde and retrograde tracers throughout these three regions. We found that there was an organized arrangement of connections between the amygdala and the PRPH cortices and that the deep (lateral, basal, and accessory basal) nuclei of the amygdaloid complex were the source of most connections between the amygdala and the PRPH cortices. The temporal polar regions of the perirhinal cortex had the strongest and most widespread interconnections with the amygdala. Connections from more caudal levels of the perirhinal cortex had a more discrete pattern of termination. Perirhinal inputs to the amygdala terminated primarily in the lateral nucleus, the magnocellular and parvicellular divisions of the basal nucleus, and the magnocellular division of the accessory basal nucleus. Return projections originated predominately in the lateral nucleus, the intermediate and parvicellular divisions of the basal nucleus, and the magnocellular division of the accessory basal nucleus. The interconnections between the amygdala and the parahippocampal cortex were substantially less robust than those with the perirhinal cortex and mainly involved the basal nucleus. Area TF was more strongly interconnected with the amygdala than was area TH. Input from the parahippocampal cortex terminated predominantly in the lateral half of the parvicellular division of the basal nucleus but also to a lesser extent in the magnocellular division of the basal nucleus and the lateral nucleus. Return projections originated predominantly in the magnocellular division of the basal nucleus and were directed almost exclusively to area TF. 

**Indexing terms: amygdala, medial temporal lobe, memory, emotion, topography, cortical connections**

The perirhinal (areas 35 and 36) and parahippocampal (areas TF and TH) cortices can be distinguished from adjacent neocortical regions by their unique cytoarchitectonic and connectional characteristics (Insausti et al., 1987; Suzuki and Amaral, 1994a,b). Studies in macaque monkeys by Jones and Powell (1970) first showed that the perirhinal and parahippocampal (PRPH) cortices are higher-order, polymodal association areas. This conclusion was based on neuroanatomical findings that the PRPH cortices received convergent unimodal sensory information from visual, auditory, and somatosensory association areas as well as polysensory information from regions within the superior temporal sulcus and the prefrontal cortex. These results were reinforced by the physiological studies of Desimone and Gross (1979), who described a subpopulation of cells in and around the PRPH cortices that responded to visual, auditory, and somatosensory stimuli. More recent neuroana-

Accepted July 2, 1996.

Address reprint requests to Dr. David G. Amaral, Center for Neuroscience, 1544 Newton Ct., University of California, Davis, Davis, CA 95616. E-mail: dgamaral@ucdavis.edu

tomical studies in monkeys have shown that the PRPH cortices not only have substantial connections with the neocortex, but they also have strong, reciprocal, and partially overlapping connections with the hippocampal formation via the entorhinal cortex (Van Hoesen and Pandya, 1975; Insausti et al., 1987; Suzuki and Amaral, 1994b). These connections, in fact, provide the major route by which cortical sensory information reaches the hippocampal formation (Insausti et al., 1987; Suzuki and Amaral, 1994b).

Although substantial attention has been focused on the relationship between the PRPH cortices and the hippocampal formation, less is known about the relationship of these cortical areas with the amygdala. The amygdala is involved in a complex array of affective functions (Weiskrantz, 1956; Jones and Mishkin, 1972; Aggleton and Passingham, 1980; Gaffan and Harrison, 1987; LeDoux, 1987; Gallagher and Chiba, 1996; McGaugh et al., 1992; Murray et al., 1996). Its damage produces a wide range of behavioral changes including hyperorality, passivity, alterations of food preferences, and loss of social rank (Rosvold et al., 1954; Weiskrantz, 1956; Aggleton and Passingham, 1980; Murray et al., 1996), as well as impairments in appetitive and aversive conditioning (Weiskrantz, 1956; for review, see Davis, 1992; Kesner, 1992; McGaugh et al., 1992; and LeDoux, 1995). Recent behavioral experiments in monkeys and rats support the idea that the amygdala and at least some parts of the perirhinal cortex subserve related functions. Lesions that involve the perirhinal cortex in monkeys produce profound emotional changes that are similar to those associated with amygdalectomy (Kling et al., 1993).

Consistent with these behavioral results, neuroanatomical studies in monkeys demonstrated the presence of interconnections between the amygdala and the PRPH cortices. Whitlock and Nauta (1956) showed that rostral temporal lobe regions encompassing the perirhinal cortex projected to the amygdala. Aggleton et al. (1980) added to this finding by demonstrating a fairly substantial projection to the amygdala from the temporal polar portion of the perirhinal cortex but weaker projections from more caudal portions of the PRPH cortices. Van Hoesen (1981) reported projections from area 35 of the perirhinal cortex to the basal and accessory basal nuclei and from the parahippocampal cortex to the central and basal nuclei. Prominent return projections from the amygdala are directed to the temporal polar portion of the perirhinal cortex, with substantially weaker projections to more caudal regions of the perirhinal cortex and to the parahippocampal cortex (Amaral and Price, 1984). Saunders and Rosene (1988) reported that the lateral nucleus of the rhesus monkey originates few if any projections to the perirhinal cortex, whereas the basal and accessory basal nuclei contribute more significant inputs.

Despite these important contributions to our understanding of amygdala-PRPH connections, the precise topographic organization of PRPH connections with the amygdala has not been clearly established. It is not clear, for example, whether the same regions of the PRPH cortices project both to the amygdala and to the hippocampal formation. Nor has there been a clear estimate of the relative magnitude of PRPH connections to each of these prominent medial temporal lobe regions. To examine in more detail the organization of amygdala connections with the PRPH cortices in macaque monkeys, we placed anterograde and retrograde tracers throughout these three areas. Specifically, we sought to determine (1) the magnitude and regional topography of amygdala-PRPH connections and, in particular, whether there were any preferential connections, and (2) whether the organization of inputs and outputs was complementary to, or overlapping with, those between the PRPH cortices and the hippocampal formation.

*Abbreviations*

| | |
|---|---|
| AAA | anterior amygdaloid area |
| AB | accessory basal nucleus |
| ABmc | accessory basal nucleus, magnocellular division |
| ABpc | accessory basal nucleus, parvicellular division |
| AHA | amygdalohippocampal area |
| B | basal nucleus |
| Bi | basal nucleus, intermediate division |
| Bmc | basal nucleus, magnocellular division |
| Bpc | basal nucleus, parvicellular division |
| CE | central nucleus |
| CEl | central nucleus, lateral division |
| CEm | central nucleus, medial division |
| COa | anterior cortical nucleus |
| COp | posterior cortical nucleus |
| ER | entorhinal cortex |
| I | intercalated nucleus |
| L | lateral nucleus |
| Ld | lateral nucleus, dorsal division |
| Ldi | lateral nucleus, dorsal intermediate division |
| Lv | lateral nucleus, ventral division |
| Lvi | lateral nucleus, ventral intermediate division |
| ME | medial nucleus |
| NLOT | nucleus of the lateral olfactory tract |
| PAC | periamygdaloid cortex |
| PIR | piriform cortex |
| PL | paralaminar nucleus |
| TE | area TE |
| TF | area TF of the parahippocampal cortex |
| TH | area TH of the parahippocampal cortex |

## METHODS

### Surgical procedures

Forty-four macaque monkeys (*Macaca fascicularis*) of either sex and weighing between 2.7 and 3.9 kg at the time of surgery were the subjects of these experiments. Animals were preanesthetized with ketamine hydrochloride (8 mg/kg i.m.). For experiments performed after August 1990, animals were placed on a mechanical ventilator and brought to a surgical level of anesthesia with isofluorane; for all other experiments, animals were anesthetized with Nembutal (25 mg/kg i.p.) and supplemented as necessary through a venous catheter throughout the surgery. All surgeries were performed under sterile conditions. The animals were mounted in a Kopf stereotaxic apparatus; a midline incision was made in the scalp, the dorsal skull was exposed, and the fascia and temporal muscles were displaced laterally. A craniotomy approximately 1.5 cm in diameter was made over the intended injection site with a dental drill, and the dura was reflected. The coordinates for the intended injection locations were based on the atlas by Szabo and Cowan (1984). Each injection was preceded by an electrophysiological recording of extracellular unit activity along the injection trajectory. Identification of landmarks such as areas of white matter and cortex assisted in determining the appropriate depth at which to place the injection. After the tracer was placed at the intended location (see below), the wound was closed in layers. The animal was recovered from anesthesia and then returned to its home cage. Prophylactic doses of antibiotics (claforan, 50 mg/kg, three times a day for 5 days) and analgesics (oxymorphone, 0.15 mg/kg, three times a day for 2 days) were administered.

## Retrograde tracer injections

A glass micropipette was lowered to the perirhinal cortex, the parahippocampal cortex, or the amygdaloid complex, and the fluorescent retrograde tracer Fast blue (FB; 3%) or Diamidino yellow (DY; 2%) (Dr. Illing GmbH and Co., Germany) was ejected from the pipette by air pressure (Amaral and Price, 1983). For the amygdala experiments, 500 nl of FB or 800 nl of DY was dispensed; for the cortical experiments, 500–650 nl of FB or 500–1,500 nl of DY was dispensed. Thirty retrograde tracer injections were placed in the amygdaloid complex: Unilateral injections of FB were placed in four brains; in the remaining brains, an FB or DY injection was placed in each hemisphere, for a total of two injections per brain. Twenty retrograde tracer injections were deposited at different rostrocaudal levels of the PRPH cortices. Unilateral injections of FB or DY were placed in eight animals. In the remaining experiments, FB and DY were placed at different levels of the PRPH cortices within the same hemisphere. The locations of the injection sites are illustrated in Figures 3B and 7.

## Anterograde tracer injections

For the tritiated amino acid injections, a glass micropipette was lowered to the perirhinal or the parahippocampal cortex and a 1:1 solution of $^3$H-leucine and $^3$H-proline (100 nl, concentrated to 100 μCi/μl) was ejected by air pressure. Twenty-four unilateral injections were placed at different rostrocaudal levels of the PRPH cortices. The locations of the injection sites are illustrated in Figure 3A.

## Histological procedures

After a 2-week survival period, animals were deeply anesthetized and perfused intracardially with one of two fixative solutions: *pH-shift fix*—0.9% NaCl, 0.1 M Na acetate buffer with 4% paraformaldehyde (pH 6.5), 0.1 M Na borate buffer with 4% paraformaldehyde (pH 9.5); *modified immunohistochemistry fix*—1% paraformaldehyde in 0.1 M $PO_4$ (pH 7.2), 4% paraformaldehyde in 0.1 M $PO_4$ (pH 7.2). The brain was blocked stereotaxically, postfixed in the final fixative solution for 6 hours, and then transferred to a solution of 2% dimethylsulfoxide (DMSO), 10% glycerol in 0.1 M $PO_4$ (pH 7.2) for 24 hours. The brain was transferred to a solution of 2% DMSO, 20% glycerol in 0.1 M $PO_4$ for 3 days, and then frozen in cold isopentane and stored at −70°C until cut. The frozen tissue was sectioned coronally at a thickness of 30 μm. For the retrograde study, two adjacent 1-in-8 series of sections were mounted immediately onto acid-cleaned, gelatin-coated slides and stored in the dark, desiccated, at −20°C until analyzed. For the anterograde study, a 1-in-8 series of sections was collected in a 10% solution of formalin in 0.1 M $PO_4$ (pH 7.2). The tissue was mounted onto gelatin-coated slides and processed for autoradiographic demonstration of labeled fibers and terminals according to Cowan et al. (1972). Briefly, slides were dipped in emulsion (Kodak, type NTB2), dried, and exposed in the dark, at 4°C, for 10 weeks. Slides were then developed (Kodak, D-19, 2 minutes), gently rinsed in distilled $H_2O$, fixed (Kodak, Polymax, 25% solution, 8 minutes), rinsed again, and stained by the Nissl method with thionin. An additional 1-in-8 series of sections was collected in a 10% solution of formalin in 0.1 M $PO_4$ (pH 7.2) and stained with thionin.

## Histological analysis

***Retrograde study.*** The distribution of retrogradely labeled (FB or DY) cells for all experiments was analyzed with a Leitz Dialux 20 fluorescent microscope. For experiments in which the retrograde tracer was placed in the perirhinal or the parahippocampal cortex, a 1-in-16 series of sections was analyzed throughout the amygdaloid complex. For experiments in which the retrograde tracer was placed in the amygdala, a 1-in-16 series of sections was analyzed throughout the PRPH cortices. The X-Y coordinates of the locations of retrogradely labeled cells were recorded with an MD-2 digitizer (Minnesota Datametrics, St. Paul, MN). Each file was then printed to produce a large-scale plot of the section. Camera lucida drawings of relevant cytoarchitectonic boundaries were superimposed on the plots using the adjacent Nissl-stained sections. To quantify the magnitude of the cortical projections to the amygdala and to better determine the overall projection pattern, cortical plots were subsequently "unfolded" onto two-dimensional, straight-line brain maps according to the method described by Suzuki and Amaral (1996). The density of retrogradely labeled cells throughout the cortex was normalized across cases using a percentile algorithm (see Suzuki and Amaral, 1994a), and four gray levels were designated to represent four different density levels.

***Anterograde study.*** A 1-in-16 series of autoradiograms was analyzed under brightfield and darkfield illumination with a Wild stereomicroscope and a Leitz Dialux 20 microscope for the distribution and density of anterogradely transported label within the amygdaloid complex. The profiles of labeled fibers and terminals and the cytoarchitectonic borders of amygdaloid nuclei were represented with camera lucida drawings throughout the rostrocaudal extent of the amygdala.

The data from 12 additional experiments previously described by Amaral and Price (1984) and 15 experiments described in Pitkänen and Amaral (1991; unpublished observations) were reanalyzed to confirm some of our present observations. In these experiments, 0.1–1.3 μl of tritiated amino acids or iontophoretic injections of the lectin anterograde tracer *phaseolus vulgaris* leucoagglutinine (PHA-L) were placed into different locations of the amygdaloid complex. The distribution of labeled fibers and terminals in the PRPH cortices was examined and plotted on camera lucida drawings.

# RESULTS

## Terminology

***Amygdaloid complex.*** The nuclear subdivisions of the amygdaloid complex were named according to the nomenclature proposed by Price et al. (1987) as slightly modified by Amaral and Bassett (1989) and Pitkänen and Amaral (unpublished observations). Briefly, the "deep" nuclei consist of the lateral, basal, accessory basal, and paralaminar nuclei. The lateral nucleus is composed of the dorsal, dorsal intermediate, ventral, and ventral intermediate subdivisions. The basal nucleus is subdivided into magnocellular, intermediate, and parvicellular divisions, and the accessory basal nucleus is parcelled into magnocellular, parvicellular, and ventromedial divisions. The "cortical" nuclei consist of the anterior and posterior cortical nuclei, the periamygda-

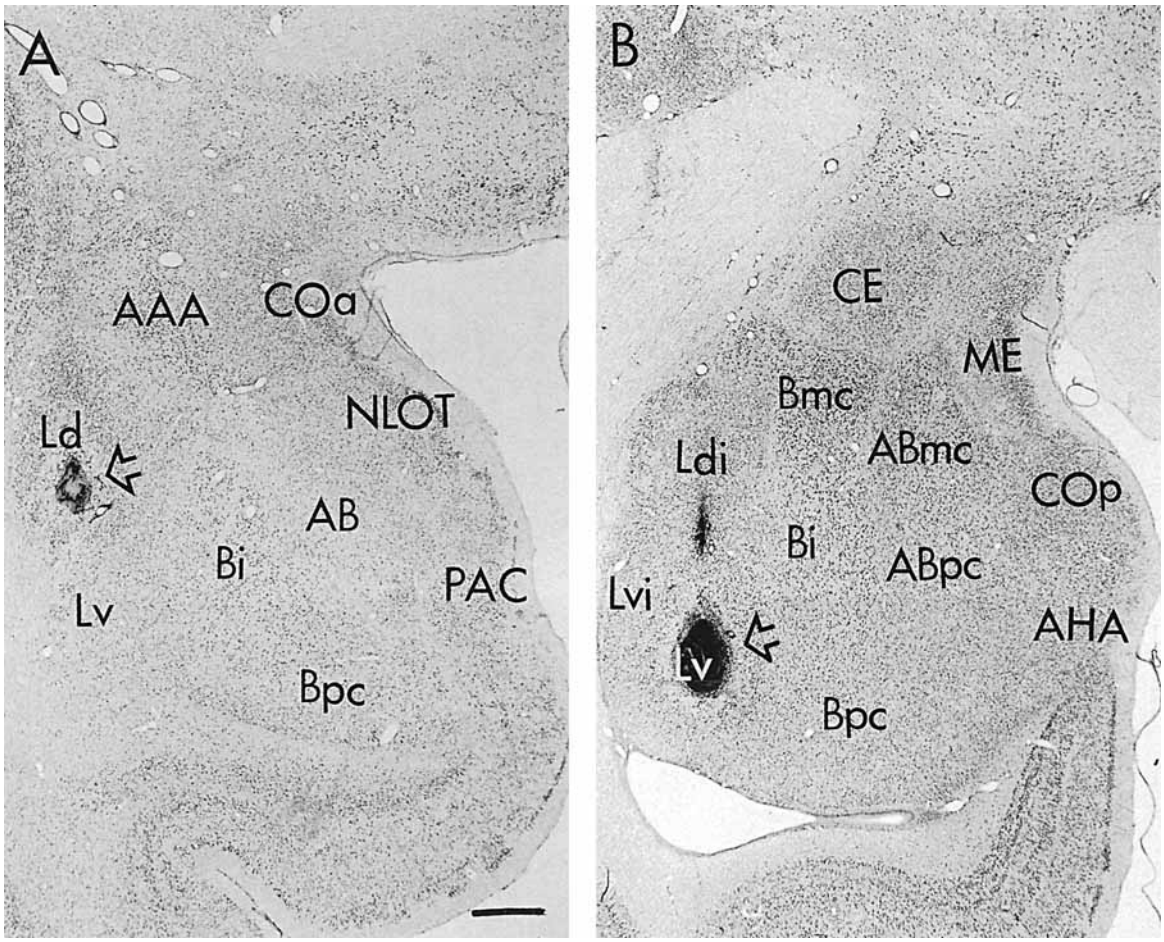


Fig. 1. Brightfield photomicrographs of Nissl-stained coronal sections through rostral (**A**) and caudal (**B**) levels of the amygdaloid complex. A is from experiment M29-92L, in which a fluorescent retrograde tracer was placed in the dorsal division of the lateral nucleus (arrow). In B, the retrograde tracer (arrow) was placed in the ventral division of the lateral nucleus (M8-92L). Scale bar = 1 mm.

loid cortex, the medial nucleus, and the nucleus of the lateral olfactory tract. "Other" nuclei are the central nucleus (medial and lateral divisions), the anterior amygdaloid area, the intercalated nuclei, and the amygdalohippocampal area. The locations of these amygdaloid nuclei are shown in Figure 1.

***PRPH cortices.*** The PRPH cortices in the macaque monkey are located on the ventromedial surface of the temporal lobe, lateral and immediately caudal to the rhinal sulcus. The PRPH cortices are named according to the nomenclature of Suzuki and Amaral (1994b) and Insausti et al. (1987). Briefly, the perirhinal cortex is composed of a narrow, medially placed area 35 and a larger, more laterally placed area 36. The most rostral portion of area 35 is located on the temporal pole. There are five subdivisions of area 36: area 36d, which lies on the temporal pole; area 36r, part of which lies on the temporal pole and which is further subdivided into areas 36rm (medial) and 36rl (lateral); and a caudally placed area 36c, which is subdivided into areas 36cl and 36cm. References to the "rostral most" or "polar" portion of the perirhinal cortex refer to those perirhinal regions that lie on the temporal pole: rostral 35, 36d, and rostral 36r. The parahippocampal cortex lies just caudal to the perirhinal cortex and is composed of two major cytoarchitectonic areas: area TH, which is medially situated and a larger area TF, which lies lateral to area TH and is made up of areas TFm (medial) and TFl (lateral). The locations and the cytoarchitecture of the PRPH cortices are shown in Figure 2.

## Organization of connections between the perirhinal cortex and the amygdaloid complex

***Projections from the perirhinal cortex to the amygdala: A summary of anterograde and retrograde experiments.*** Anterograde and retrograde tracer experiments consistently demonstrated that the perirhinal cortex generated a substantial projection to the amygdala. This projection was characterized by two major organizational features. First, there were rostrocaudal differences in the strength and extent of perirhinal input to the amygdala. The most widespread connections originated in the polar regions of the perirhinal cortex. These projections terminated predominantly in the lateral, basal, and accessory basal nuclei, with weaker projections to the anterior amygdaloid area, the anterior cortical nucleus, the nucleus of the lateral olfac-

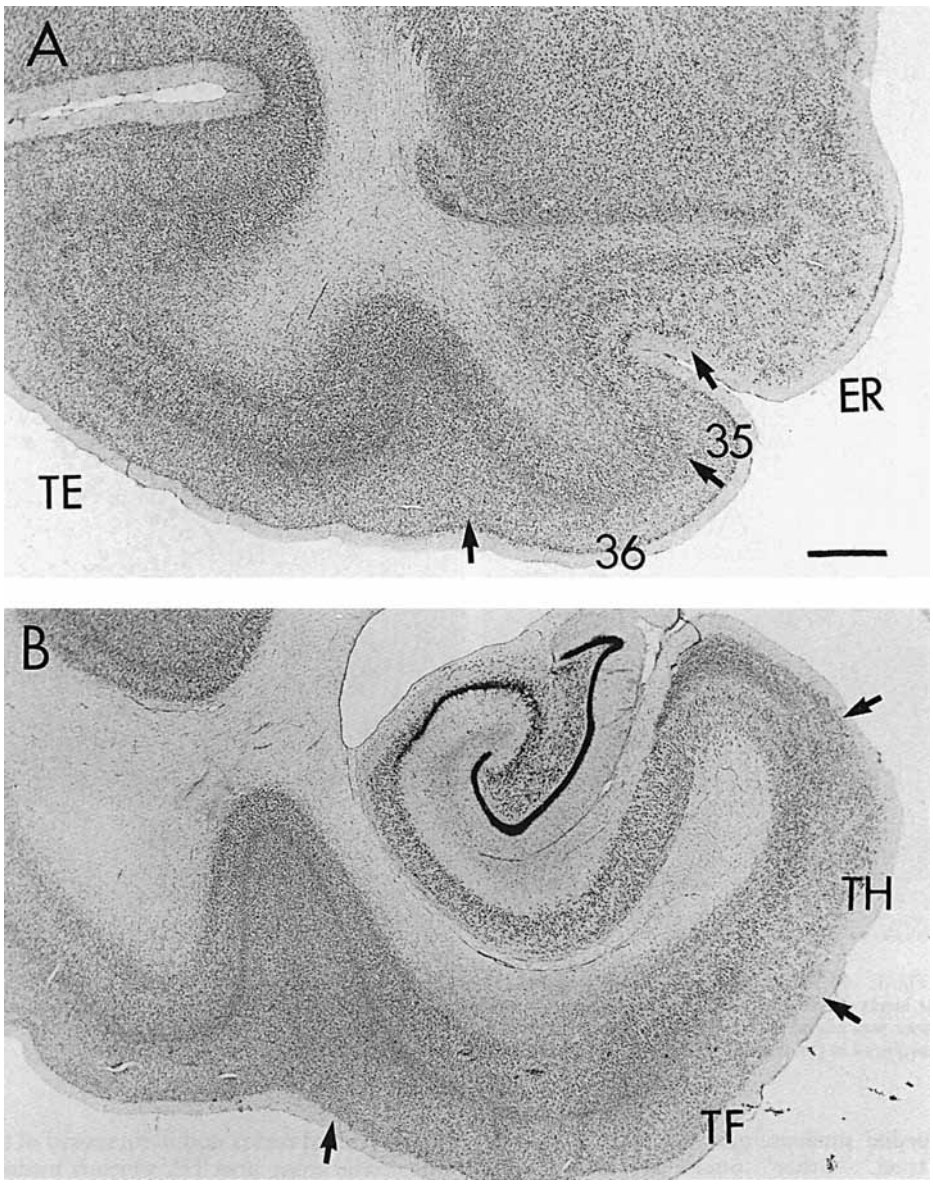


Fig. 2. Brightfield photomicrographs of Nissl-stained coronal sections through the temporal lobe, indicating the location and cytoarchitecture of areas 35 and 36 of the perirhinal cortex (**A**) and areas TF and TH of the parahippocampal (**B**) cortex. Arrows indicate boundaries between cortical subdivisions. ER, entorhinal cortex; TE, area TE. Scale bar = 1 mm.

tory tract, the periamygdaloid cortex, and the central nucleus. Projections from more caudally and ventrally situated regions of the perirhinal cortex demonstrated a more restricted termination pattern that was directed primarily to the lateral and basal nuclei. Second, perirhinal projections typically innervated subregions of each of the nuclei listed above. In the lateral nucleus, for example, the heaviest projection was directed to dorsal portions of the nucleus, whereas ventral divisions received little or no input. In the parvicellular division of the basal nucleus, the lateral aspect of the division was heavily innervated while the medial portion was considerably less innervated. In addition, input to the accessory basal nucleus was directed mainly to the magnocellular division.

Our computer-aided plotting system allowed us to evaluate the laminar organization of cortical inputs to the amygdala. The major result was that the laminar distribution of perirhinal input to the amygdala was heterogeneous, with inputs originating in both infragranular and supragranular layers. However, there appeared to be a periodic distribution of inputs from different laminae, such that across the mediolateral extent of the perirhinal cortex, there were alternating regions of infragranular inputs and supragranular inputs. These findings are now described in more detail.

***Rostrocaudal differences in perirhinal projections to the amygdala***

*Anterograde tracer studies.* The strongest projections from the perirhinal cortex to the amygdala arose from the

temporal polar region (Fig. 3). The injection in experiment DM-46 (Fig. 4) involved multiple deposits of tracer that labeled an extensive portion of areas 36d and 36r (Fig. 3). The anterogradely transported label was observed throughout the rostrocaudal extent of the amygdala and in many of its nuclei. In the lateral nucleus, the dorsal intermediate subdivision demonstrated medium to heavy innervation in the caudal half of the nucleus (Fig. 4D–F). The ventral division received a lighter input mainly in the rostral half of the nucleus (Fig. 4B,C). Only scattered silver grains were observed in the dorsal and ventral intermediate divisions. Rostral levels of the basal nucleus received heavier innervation in this case than caudal levels. For example, both the intermediate and parvicellular divisions were labeled at rostral levels of the amygdala (Fig. 4B), whereas further caudally the label was distributed more selectively to the medial aspect of the parvicellular division (Fig. 4D). There was little or no labeling of the magnocellular division of the basal nucleus from this temporal polar injection. The paralaminar nucleus received a projection that appeared to be continuous with the labeling of the parvicellular division of the basal nucleus (Fig. 4A,B). The accessory basal nucleus received the heaviest projection, which was distributed to all rostrocaudal levels and all divisions of the nucleus; the magnocellular division demonstrated a slightly higher density of label than other parts of the nucleus (Fig. 4D–F). Of the projections to other amygdaloid nuclei or areas, the most prominent was to the periamygdaloid cortex, which demonstrated moderate-to-heavy labeling of all its divisions (Fig. 4A–E). There were also lighter projections to the anterior amygdaloid area, the anterior and posterior cortical nuclei, the medial nucleus, the amygdalohippocampal area and the nucleus of the lateral olfactory tract.

One of the temporal polar injections (M22-91) more heavily involved area 35 than in experiment DM-46 (Fig. 3). In general, the pattern of labeling in both cases was very similar. However, it appeared that the labeling of the central nucleus, the anterior cortical nucleus, and the medial nucleus was somewhat heavier in the case of the area 35 injection.

There were both regional and intranuclear changes in the pattern of amygdaloid labeling resulting from injections at successively more caudal levels of areas 35 and 36. These changes are summarized by comparing experiment DM-46 (Fig. 4) with two experiments illustrated in Figures 5 and 6. Experiment M5-94 (Fig. 5) had an injection located in the polar region of areas 35 and 36 but was more ventrally and caudally placed than the injection in experiment DM-46 (Fig. 4). The injection in experiment M1-92 (Fig. 6) was even more caudally placed, at the border of areas 36r and 36c (Fig. 3). One difference in the patterns of labeling relates to the rostrocaudal level of the lateral nucleus that was innervated. The most rostral (polar) portion of the perirhinal cortex tended to innervate more caudal levels of the lateral nucleus (Fig. 4D–F); a more caudally placed perirhinal injection most heavily innervated mid levels of the lateral nucleus (Fig. 5C,D); and an even more caudal injection resulted in labeling mainly over the rostral half of the lateral nucleus (Fig. 6A). Thus, there was an inverse rostrocaudal topography.

There was an even more striking change in the distribution of input to the basal nucleus. Although the polar injection (DM-46) gave rise to little or no input to the magnocellular division of the basal nucleus (Fig. 4D–F), the most caudal perirhinal injection resulted in a substantial input to this division of the basal nucleus (Figs. 6D–F, 9A,B). A more subtle shift was seen in the parvicellular division of the basal nucleus. The rostral perirhinal injections primarily innervated the medial aspects of this division, whereas the caudal perirhinal injections innervated more lateral portions (cf. Figs. 4D,E, 5C,D vs. Fig. 6B,C). By contrast, the magnocellular division of the accessory basal nucleus received a much heavier input from the rostral, polar regions of the perirhinal cortex than from more caudal levels (cf. Figs. 4D–F vs. 6D–F). Finally, compared with polar regions of the perirhinal cortex, caudal perirhinal regions originated more meager projections to the other amygdaloid nuclei, such as the periamygdaloid cortex and the central nucleus.

*Retrograde tracer studies.* The retrograde tracer studies not only confirmed many of the patterns of perirhinal projections to the amygdala but also contributed additional information on the regional origins of these projections. As illustrated in Figure 11, retrogradely labeled cells were observed throughout the perirhinal cortex after injections into the amygdaloid complex. When the injection was placed into rostral levels of the lateral nucleus, the heaviest densities of retrogradely labeled cells were in both the polar and the ventrocaudal portions of area 36r (Fig. 11A,B). However, when the injection was placed more caudally in the lateral nucleus, the retrograde labeling was observed predominantly in the temporal polar portion of the perirhinal cortex (Fig. 11C,D).

When retrograde tracer injections were placed into the accessory basal nucleus, the heaviest density of retrograde labeling was in the temporal polar portion of perirhinal cortex and a lower density of cells was observed in more ventrocaudal divisions of the perirhinal cortex (Fig. 11E). Consistent with the relatively meager anterograde projections that we observed to the parvicellular division of the accessory basal nucleus (Figs. 4–6), a retrograde tracer injection focused in the parvicellular division of the accessory basal nucleus led to far fewer labeled cells in the perirhinal cortex than the injection into the magnocellular division (cf. Fig. 11E,F). Although we have no cases with selective injections of the magnocellular division of the basal nucleus, a reanalysis of a previously reported experiment (Amaral and Insausti, 1992) provided some confirmation for the present findings. In experiment M1-87, an injection of wheat germ agglutinin-horseradish peroxidase (WGA-HRP) was deposited into the amygdala and focused in the magnocellular and intermediate divisions of the basal nucleus. Although a moderate number of retrogradely labeled cells was observed in the polar regions of the perirhinal cortex, a comparatively stronger projection originated from more ventral and caudal regions.

One of the deficiencies of the anterograde tracer experiments was that we were unable to determine clearly the relative contributions of projections originating in areas 35 and 36; the retrograde tracer studies partially rectified this deficiency. When retrograde tracer injections were located in the lateral nucleus, labeled cells were distributed within both areas 35 and 36. However, the density of labeled cells was often greater in area 36 than in area 35. Areas 35 and 36 also both project to the accessory basal nucleus, and in this case the densities of labeled cells appeared more equal (Fig. 11E,F).

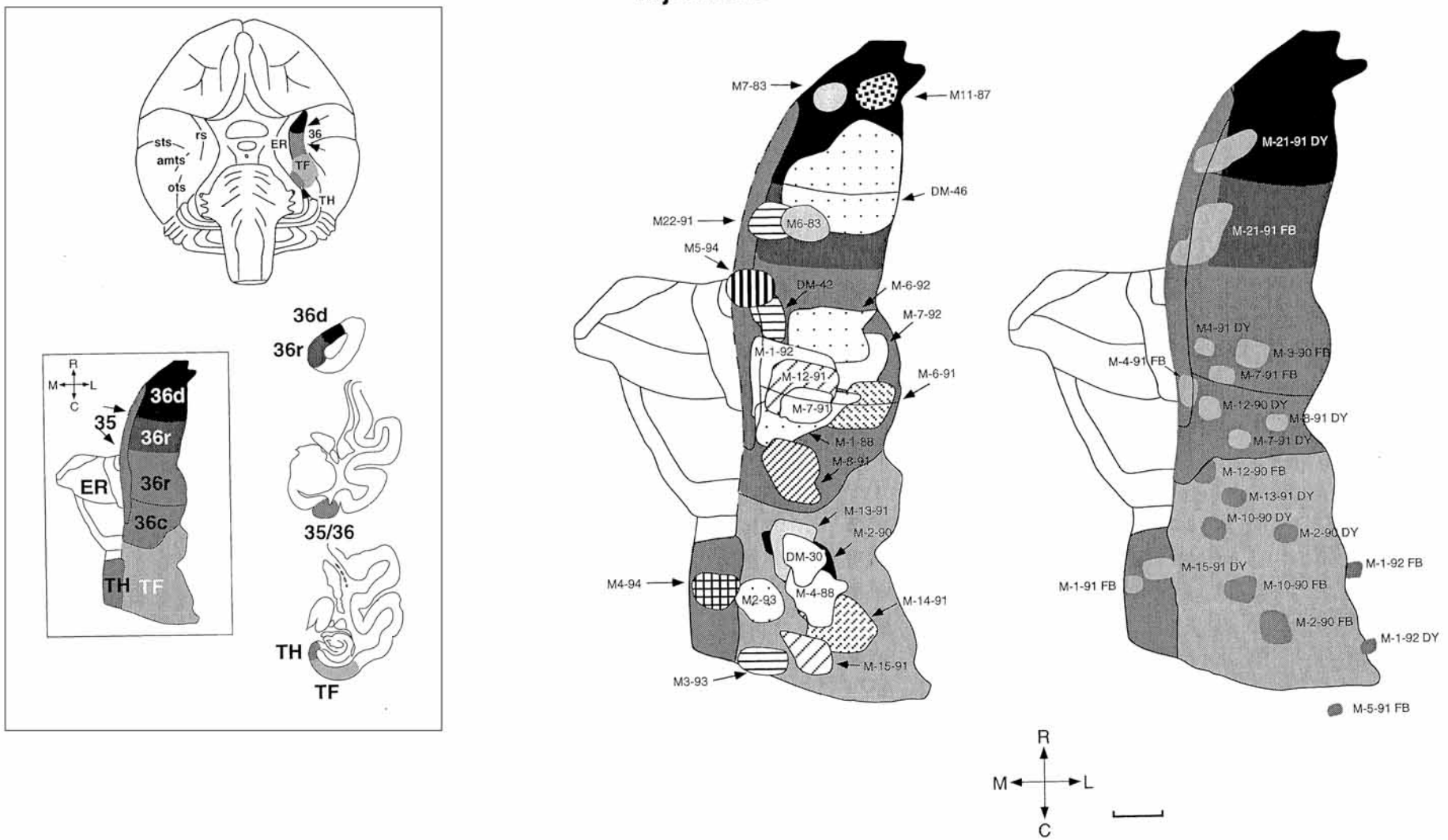


Fig. 3. Locations of cortical tracer injections. Box at left shows a ventral view of a macaca fascicularis monkey brain (top), a representative unfolded two-dimensional map of the entorhinal, perirhinal (areas 35, 36d, 36r, 36c), and parahippocampal (areas TF and TH) cortices (bottom left), and three coronal sections through different rostrocaudal levels of the temporal lobe (bottom right). The locations of the perirhinal and parahippocampal cortices are coded by different shades of gray. **A:** An unfolded map that shows the locations of the 24 cortical $^{3}$H-amino acid injections that were analyzed for this study. **B:** An unfolded map that shows the locations of the 19 cortical retrograde tracer injections that were analyzed for this study. R, rostral; C, caudal; M, medial; L, lateral. Scale bar = 2 mm (applies only to the unfolded maps).

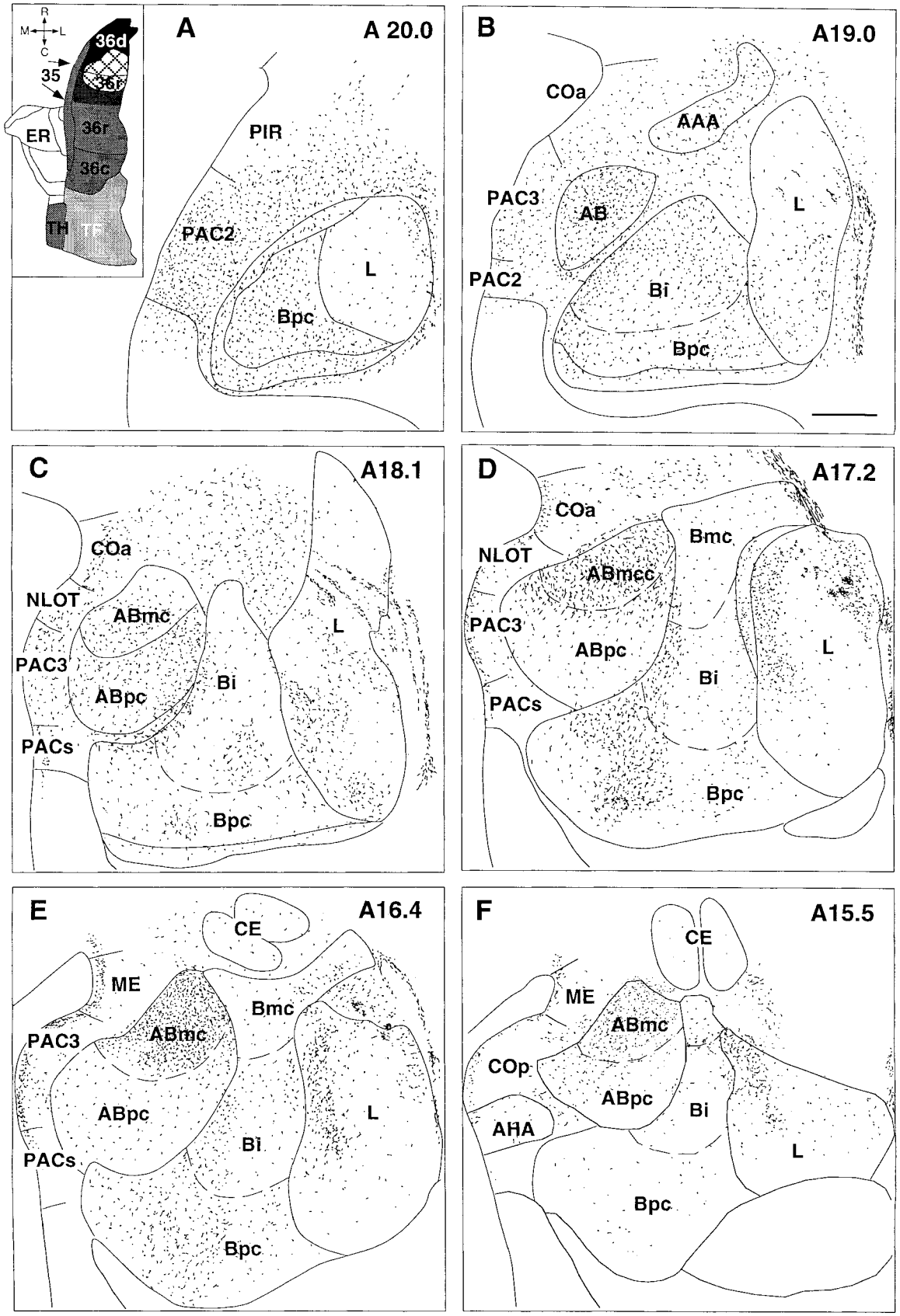


Fig. 4. Camera lucida drawings through six levels of the amygdala, arranged from rostral (**A**) to caudal (**F**), showing the distribution of anterogradely transported fibers and terminals resulting from a $^{3}$H-amino acid injection that was placed in the rostral portion of area 36, on the temporal pole (area 36r, experiment DM-46). There was substantial termination throughout most of the amygdaloid nuclei with the exception of the magnocellular division of the basal nucleus, which received only meager projections. R, rostral; C, caudal; L, lateral, M, medial. Scale bar = 1.0 mm and applies to A–F.

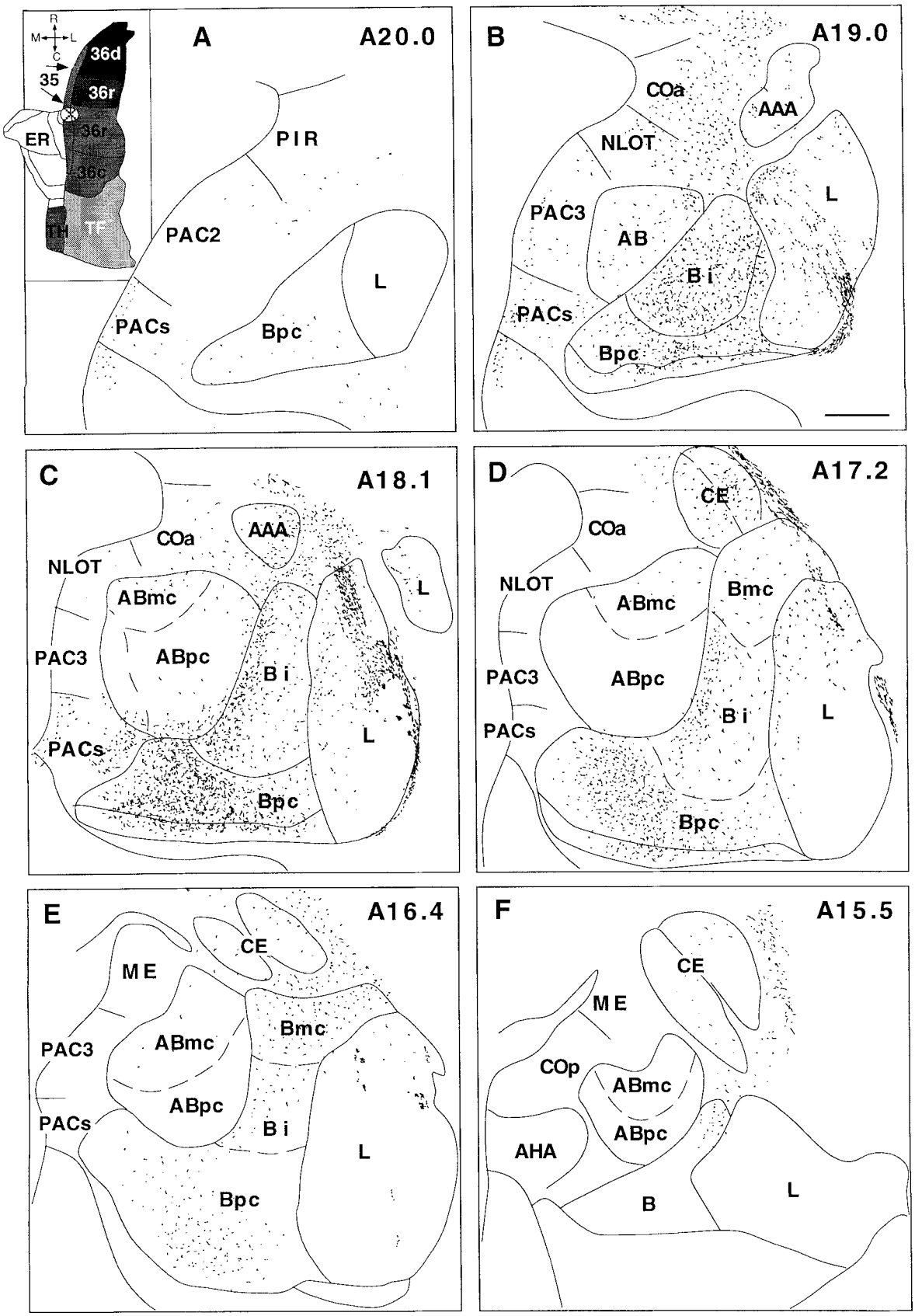


Fig. 5. Camera lucida drawings through six levels of the amygdala, arranged from rostral (**A**) to caudal (**F**), showing the distribution of anterogradely transported fibers and terminals after a $^{3}$H-amino acid injection was placed in the ventral portion of areas 35 and 36r (experiment M5-94). Projections were directed to the lateral nucleus (B–D), the parvicellular division of the basal nucleus (B–D), and the magnocellular division of the basal nucleus (D–F). R, rostral; C, caudal; L, lateral; M, medial. Scale bar = 1.0 mm and applies to A–F.

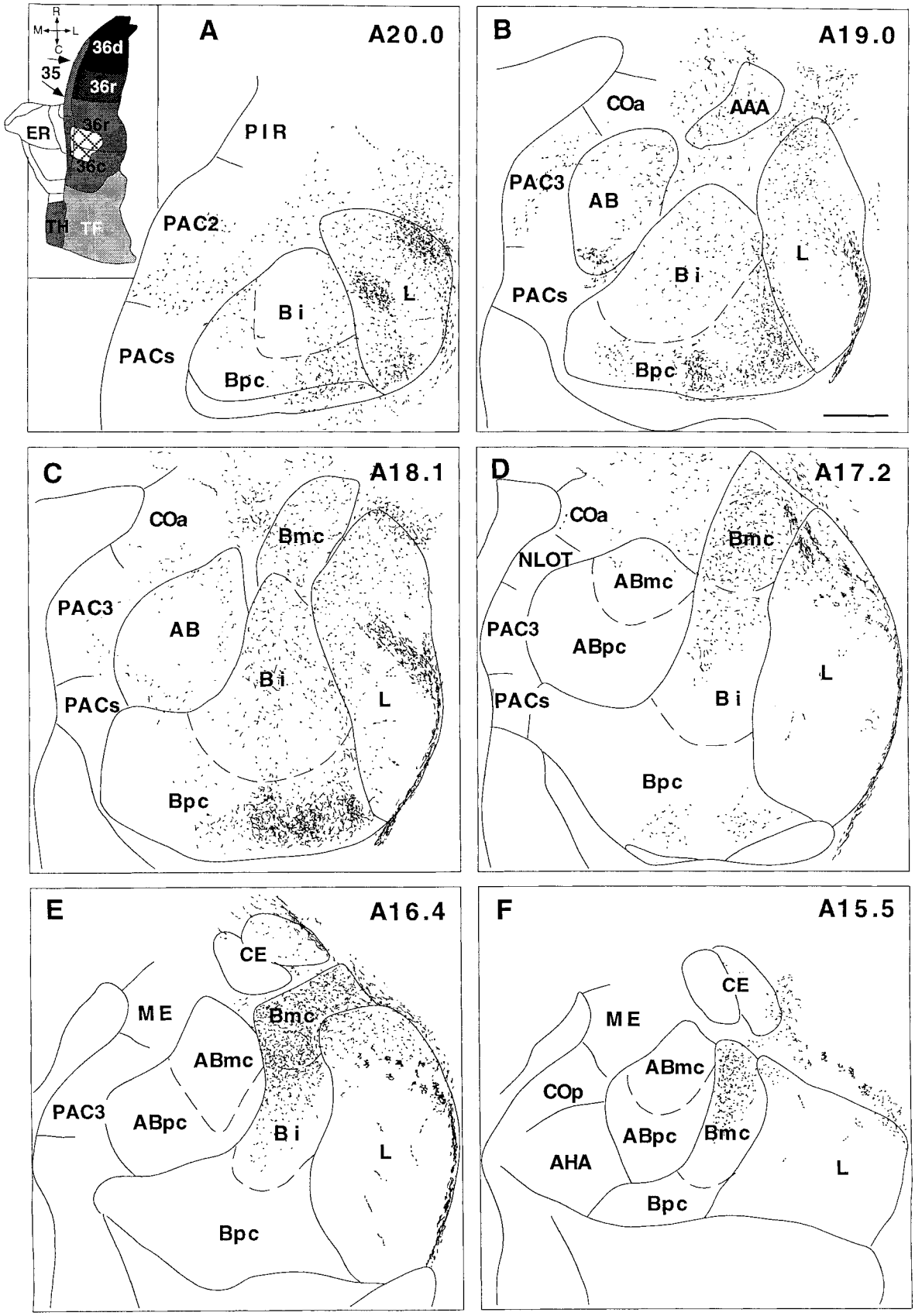


Fig. 6. Camera lucida drawings through six levels of the amygdala, arranged from rostral (**A**) to caudal (**F**), showing the distribution of anterogradely transported fibers and terminals after a $^{3}$H-amino acid injection was placed in the ventral portions of areas 35, 36r, and 36c (experiment M1-92). Substantial projections were directed to the lateral nucleus (A–C), the parvicellular division of the basal nucleus (A–C), and the magnocellular division of the basal nucleus (D–F). R, rostral; C, caudal; L, lateral; M, medial. Scale bar = 1.0 mm and applies to A–F.

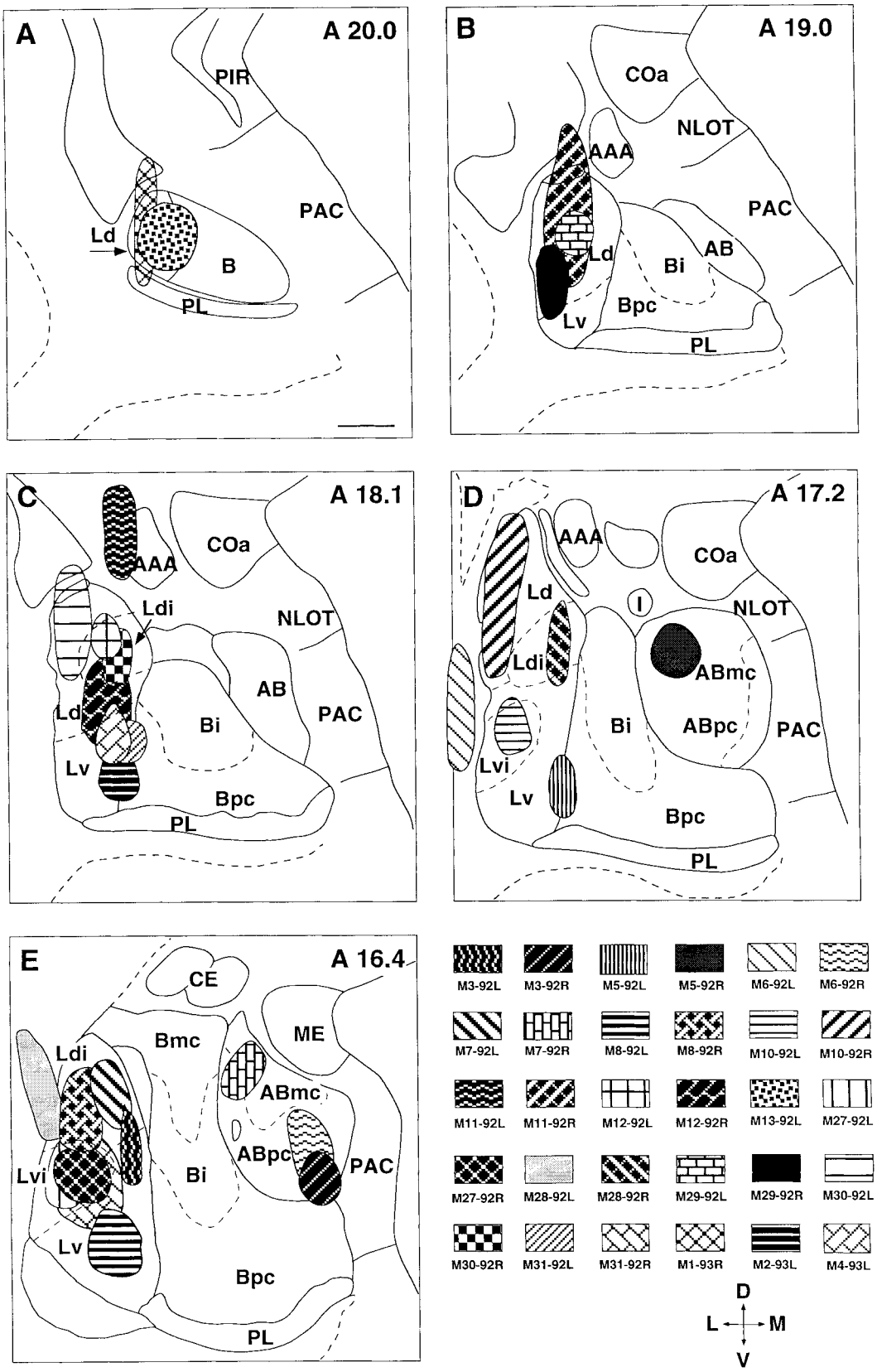


Fig. 7. Locations of retrograde dye injections in the amygdaloid complex. Injections are plotted on five representative coronal levels of the amygdala, arranged from rostral (**A**) to caudal (**E**). Shaded patterns indicate the shape and size of individual injection sites. D, dorsal; V, ventral; L, lateral; M, medial. Scale bar = 1.0 mm and applies to A–E.

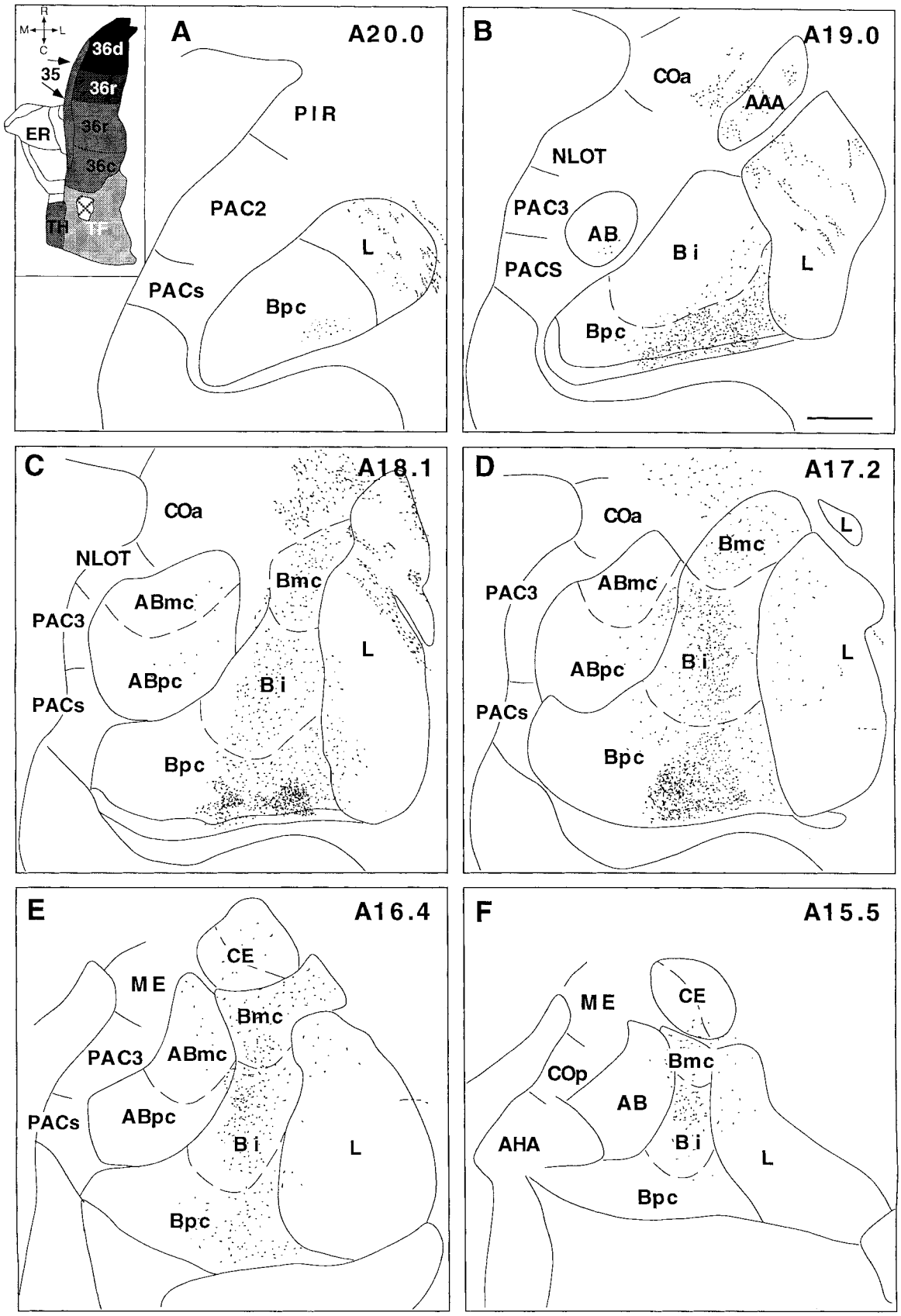


Fig. 8. Camera lucida drawings through six levels of the amygdala, arranged from rostral (**A**) to caudal (**F**), showing the distribution of anterogradely transported fibers and terminals after a $^{3}$H-amino acid injection was placed in area TF of the parahippocampal cortex (experiment M13-91). Input was directed mostly to the basal nucleus, especially the parvicellular division (B–D). R, rostral; C, caudal; L, lateral; M, medial. Scale bar = 1.0 mm and applies to *A–F*.

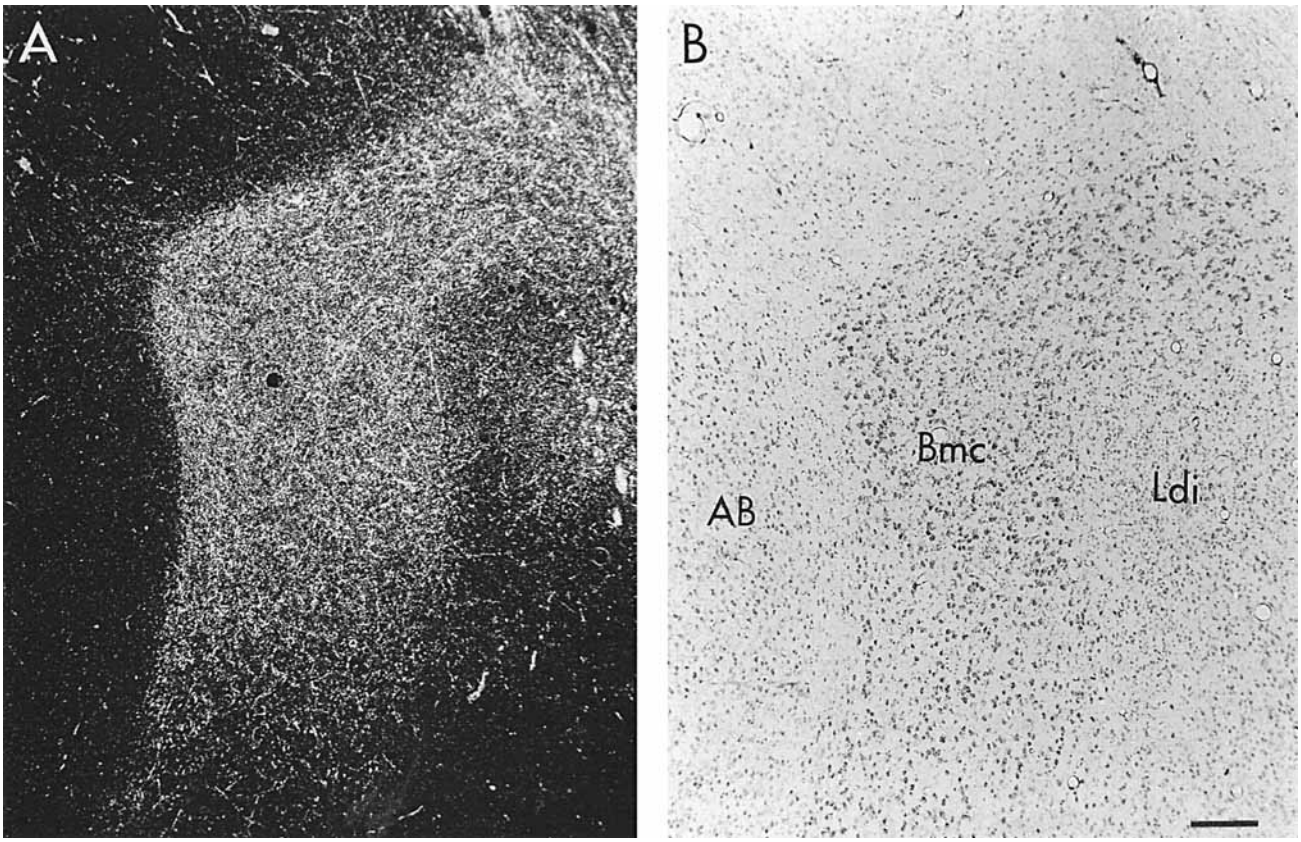


Fig. 9. **A:** Darkfield photomicrograph of a coronal section through the amygdaloid complex demonstrating anterogradely transported fibers and terminals in the magnocellular division of the basal nucleus after a $^{3}$H-amino acid injection was placed in areas 35 and 36 of the perirhinal cortex (experiment M1-92). **B:** Brightfield photomicrograph of the same section to indicate the borders of the basal nucleus. Scale bar = 250 μm in B and also applies to A.

***Perirhinal input is distributed differentially to each amygdaloid area.*** A second feature of the perirhinal projection to the amygdaloid complex was that the termination fields within the amygdala were quite heterogeneous, although some divisions of amygdaloid nuclei receive topographically organized projections from the perirhinal cortex. The parvicellular division of the basal nucleus, for example, is innervated laterally by the ventrocaudal portion of the perirhinal cortex (Fig. 6A–C) and medially by the temporal polar perirhinal cortex (Figs. 4D,E, 5C,D).

In the lateral nucleus, terminal fields from the different divisions of the perirhinal cortex were observed in the dorsal and dorsal intermediate divisions, most densely at rostral levels of the dorsal division (Fig. 6A). Little or no labeling was seen in the ventral and ventral intermediate divisions, especially at caudal levels. Here, the retrograde data are somewhat at variance with the anterograde material. Retrograde injections that involved the dorsal and dorsal intermediate divisions of the lateral nucleus led to widespread and heavy labeling throughout the perirhinal cortex (Fig. 11A,B). However, when a retrograde tracer was placed into the ventral intermediate (Fig. 11C) or ventral (Fig. 11D) division of the lateral nucleus, the same region where we saw little anterograde tracer labeling, there were fairly high densities of retrogradely labeled cells in the temporal polar perirhinal cortex. Interestingly, in the case with the ventral division injection, there were very few retrogradely labeled cells in the ventrocaudal portions of the perirhinal cortex. The fluorescent tracers that we used can be retrogradely transported by fibers of passage as well as by axon terminals. Thus, some of the retrogradely labeled cells in the perirhinal cortex may have had axons that passed through but did not terminate at the locus of the amygdala injection site, and amygdala-perirhinal projections might have been overestimated by the retrograde data. The confirmation of a polar perirhinal projection to the ventral division of the lateral nucleus awaits further anterograde tracer experiments.

In summary, most of the major nuclei of the amygdala received an input from some portion of the perirhinal cortex. The magnitude and extent of topographic organization of these inputs varied substantially from nucleus to nucleus and from division to division within a nucleus.

***Laminar organization of perirhinal projections to the amygdala.*** Because the positions of retrogradely cells were accurately plotted and the numbers of labeled cells per defined cortical area could be determined, it was possible to carry out a quantitative analysis of the laminar distribution of perirhinal neurons that projected to the amygdala. To simplify this analysis somewhat, we subdivided the perirhinal cortex into equidistant columns (77 μm wide) along layer IV on the coronal data plots. For each column, we counted the number of cells above and below layer IV. We then created an unfolded map of the cortex and assigned

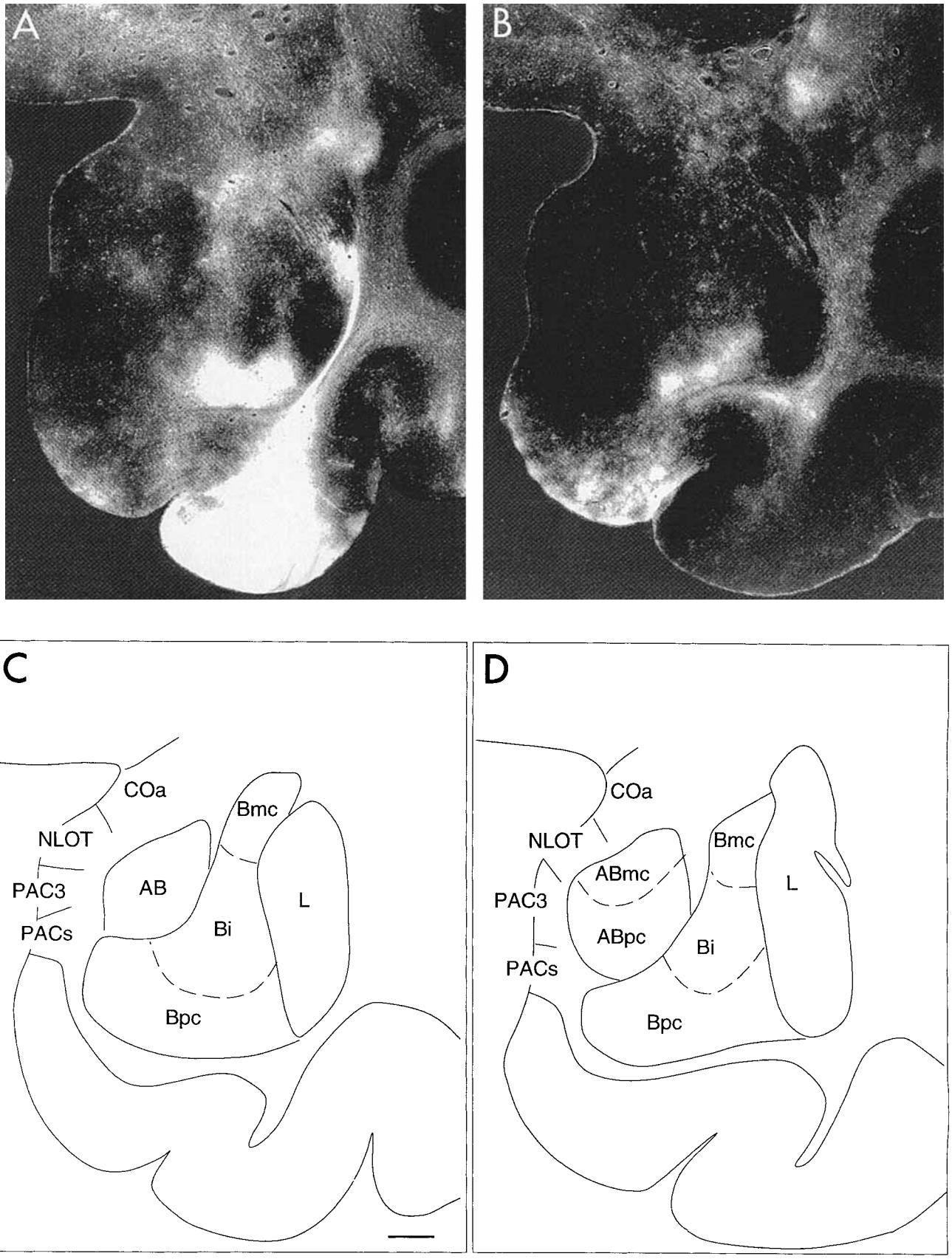


Fig. 10. Darkfield photomicrographs of coronal sections through similar levels of the amygdaloid complex for experiments in which $^{3}$H-amino acids were placed in areas 35 and 36 of the perirhinal cortex (**A,** experiment M1-92) and area TF of the parahippocampal cortex (**B,** experiment M13-91). Both cortical areas contributed substantial projections to the parvicellular division of the basal nucleus. **C, D:** Cytoarchitectonic boundaries for A and B, respectively. Scale bar = 1.0 mm and applies to A–D.


Fig. 11. Two-dimensional, unfolded density maps that show the origin of perirhinal and parahippocampal inputs to different regions of the lateral nucleus (**A–D**) and the accessory basal nucleus (**E,F**). The maps illustrate a portion of the temporal lobe extending from the entorhinal cortex (medially) to the fundus of the superior temporal sulcus (laterally). Different shades of gray represent the strength of projections to the amygdala: black, high; dark gray, medium to high; gray, medium to low; light gray, low. Box to the right of each map indicates the experiment number and shows the location of the retrograde tracer injection in the lateral (A–D) or accessory basal (E,F) nucleus. Cytoarchitectonic areas and structural landmarks are indicated on each map. Orientation arrows (R, rostral; C, caudal; M, medial; L, lateral) apply to unfolded maps only.

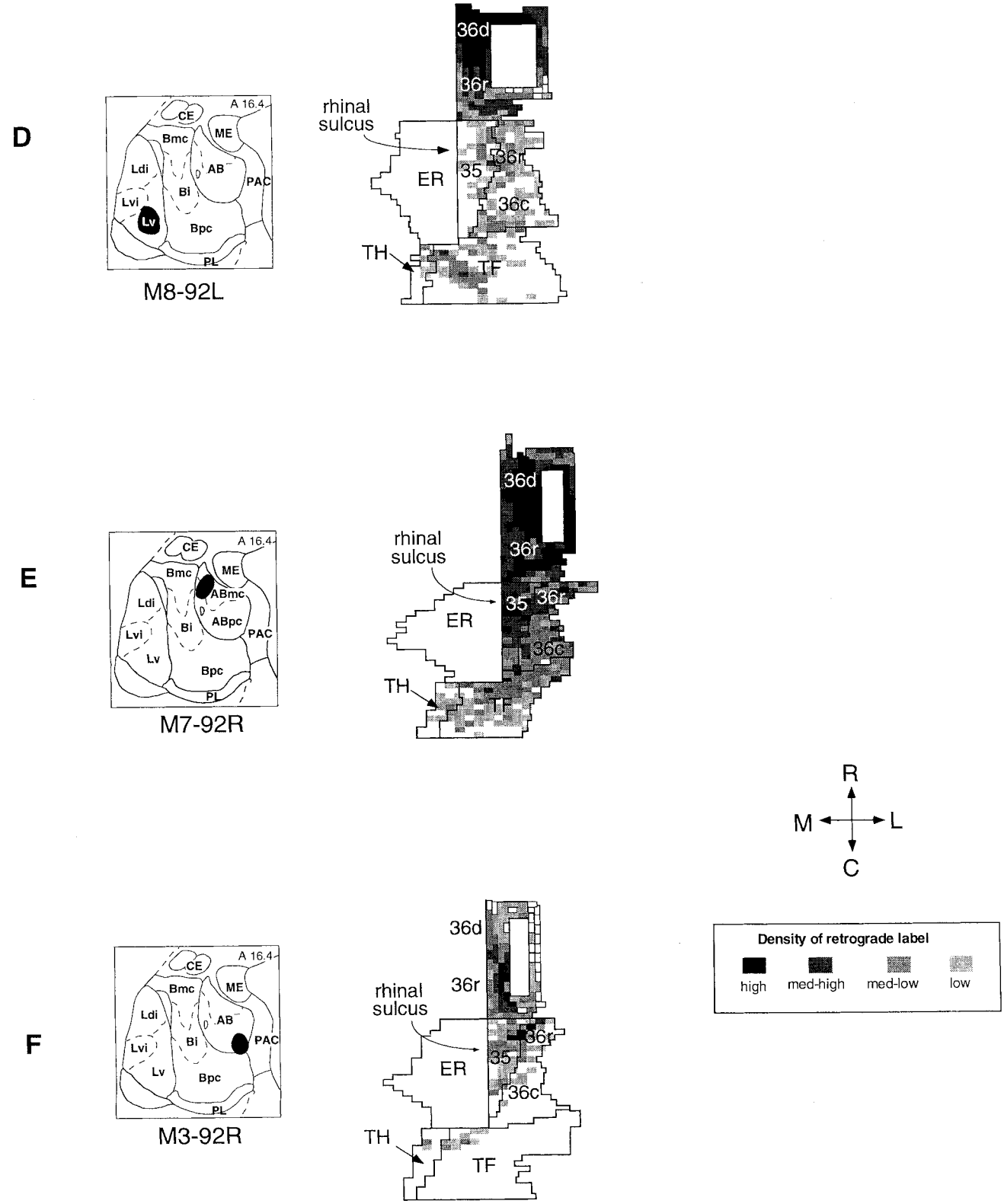
D
A 16.4
CE
Bmc
ME
Ldi
AB
PAC
Bi
Lvi
Lv
Bpc
PL
M8-92L
36d
36r
rhinal sulcus
35
36r
ER
36c
TH
TF
E
A 16.4
CE
Bmc
ME
ABmc
Ldi
ABpc
Bi
PAC
Lvi
Lv
Bpc
PL
M7-92R
36d
rhinal sulcus
36r
35
36r
ER
36c
TH
TF
R
M
L
C
Density of retrograde label
high
med-high
med-low
low
F
A 16.4
CE
Bmc
ME
Ldi
AB
Bi
PAC
Lvi
Lv
Bpc
PL
M3-92R
36d
rhinal sulcus
36r
36r
35
ER
36c
TH
TF

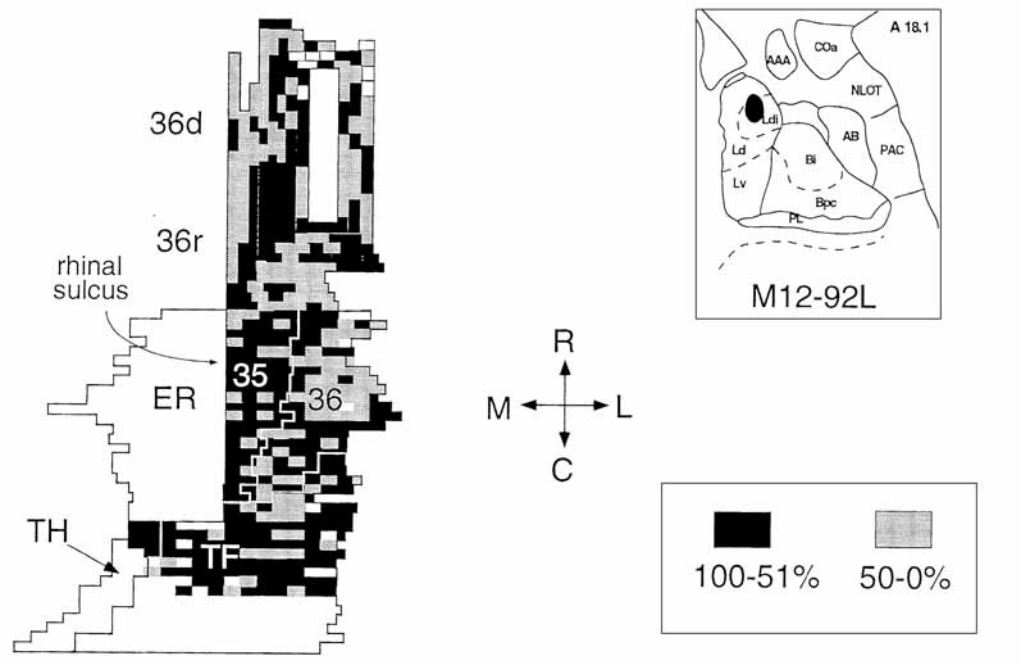


Fig. 12. Two-dimensional unfolded density map that shows the laminar distribution of perirhinal and parahippocampal input to the lateral nucleus. Conventions as in Figure 11, *except* that shading patterns indicate the percentage of retrogradely labeled cells in the infragranular layers: black, 100–51% cells in infragranular layers; light gray, 50–0%. R, rostral; C, caudal; M, medial; L, lateral.

gray values to each column based on whether most cells were in the infragranular layers (black) or in the supragranular layers (gray). The results of one of these analysesis shown in Figure 12. It is immediately apparent that the perirhinal cells that project to the amygdala are located both in infragranular and in supragranular layers. In some regions, such as area 35, most of the labeled cells appeared to be in the infragranular layers. However, in area 36, there appeared to be patches of cortex that had predominantly superficial versus deep labeling and other patches that had predominant deep labeling. These periodic patches of deep versus superficial labeling continued into the laterally adjacent area TE. Although we believe that the observation of this patch-like organization is reliable, its functional significance is not clear.

***Projections from the amygdala to the perirhinal cortex: A summary of anterograde and retrograde tracer experiments.*** The organization of the projections from the amygdala to the perirhinal cortex was similar to that of perirhinal-amygdala projections and demonstrated two major characteristics. First, like the perirhinal-amygdala projections, the amygdala-perirhinal projection pattern demonstrated a rostrocaudal gradient. The heaviest amygdaloid projection was directed to the polar portion of the perirhinal cortex and arose from widespread areas of the amygdala, but especially the deep nuclei. Projections to progressively more ventral and caudal portions of the perirhinal cortex decreased substantially and in a graded fashion such that input to the most caudal regions of the perirhinal cortex were weak and originated almost exclusively in the lateral nucleus. An exception was the input from the parvicellular and intermediate divisions of the basal nucleus to area 35, which were robust even at caudal levels of the perirhinal cortex. Second, the different amygdaloid nuclei, and even their subdivisions, demonstrated unique patterns of input to the perirhinal cortex. This heterogeneous connectivity was reminiscent of perirhinal-amygdala projections. The lateral nucleus contributed the greatest proportion of input to areas 36d and 36c whereas the parvicellular and intermediate divisions of the basal nucleus projected most strongly to area 36r. The magnocellular division of the basal nucleus did not project significantly to any regions of the perirhinal cortex. Additional significant projections arose from the accessory basal nucleus, particularly the magnocellular and ventromedial subdivisions, and the periamygdaloid cortex.

***Rostrocaudal gradient of amygdala projections to the perirhinal cortex.*** The amygdala projected much more heavily to rostral regions of the perirhinal cortex than to caudal regions. In addition, the origin of amygdala projections was more widespread to the rostral versus the caudal perirhinal cortex. This is perhaps most easily appreciated by summarizing the results of a series of retrograde tracer experiments (Figs. 13–16). In these experiments, an injection of fluorescent dyes was injected either into area 36d (Fig. 13), polar area 36r (Fig. 14), ventral area 36r (Fig. 15), or area 36c (Fig. 16). It is immediately apparent that the number of retrogradely labeled cells was substantially larger after the rostral, polar injections (Figs. 13, 14) and relatively meager after the more caudally placed area 36c injection (Fig. 16). To investigate these differences more quantitatively, we counted the number of retrogradely labeled cells in each nucleus at 480-μm sampling intervals (every other section) throughout the amygdaloid complex.

The quantitative analyses support the qualitative impression gained from Figures 13–16. In the injections of areas 36d and polar 36r, the number of cells counted in the lateral nucleus was 4,197 and 2,181, respectively. However, when injections were placed in areas 36r and 36c, the number of

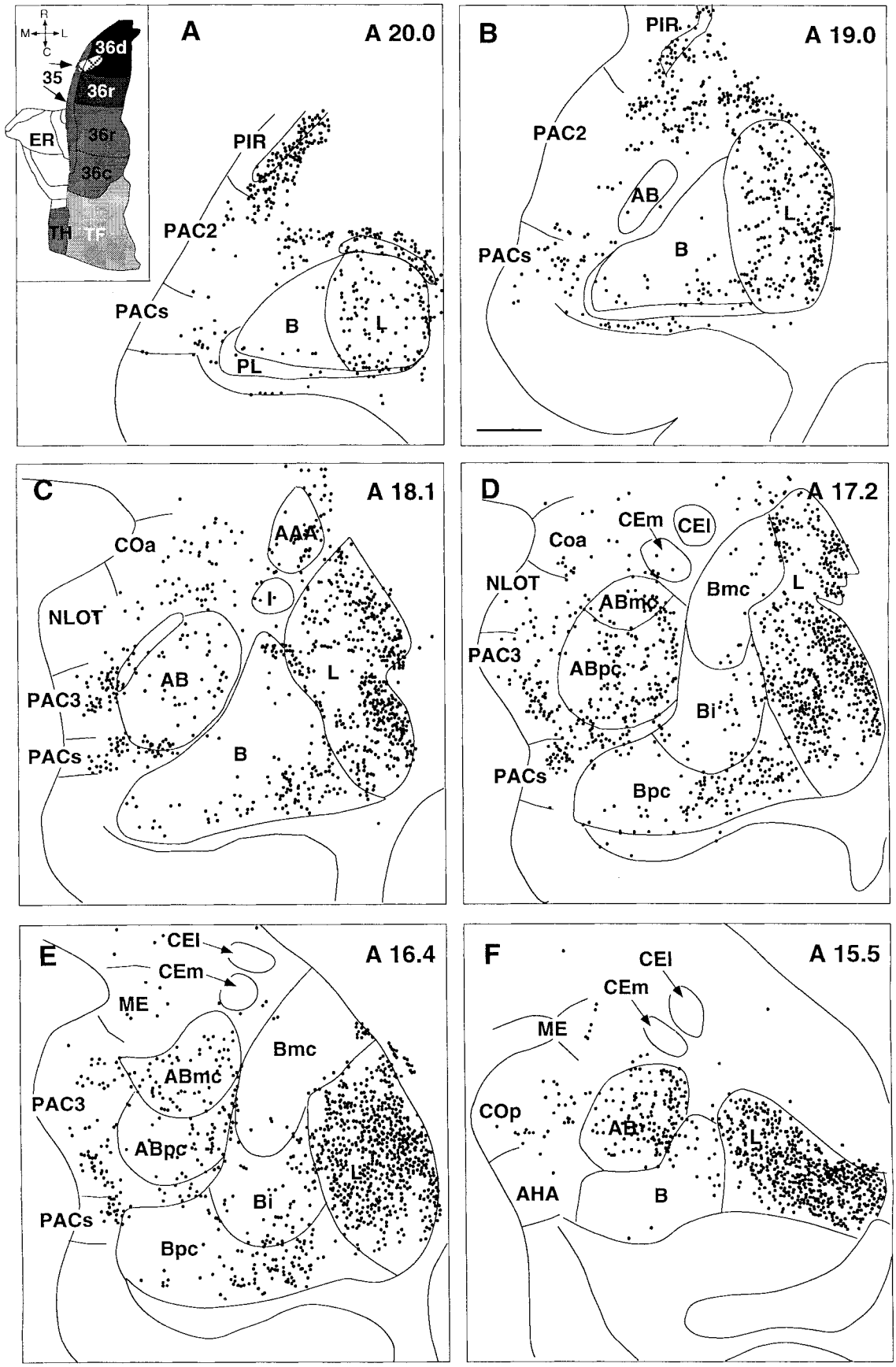


Fig. 13. Line drawings through six levels of the amygdala, arranged from rostral (**A**) to caudal (**F**), that show the distribution of retrogradely labeled cells after the retrograde tracer Diamidino yellow was placed in area 36d of the perirhinal cortex (experiment M21-91 DY). The densest projections arose from the lateral nucleus, especially its caudal levels, whereas projections from the basal nucleus were considerably weaker. R, rostral; C, caudal; M, medial; L, lateral. Scale bar = 1.0 mm and applies to A–F.

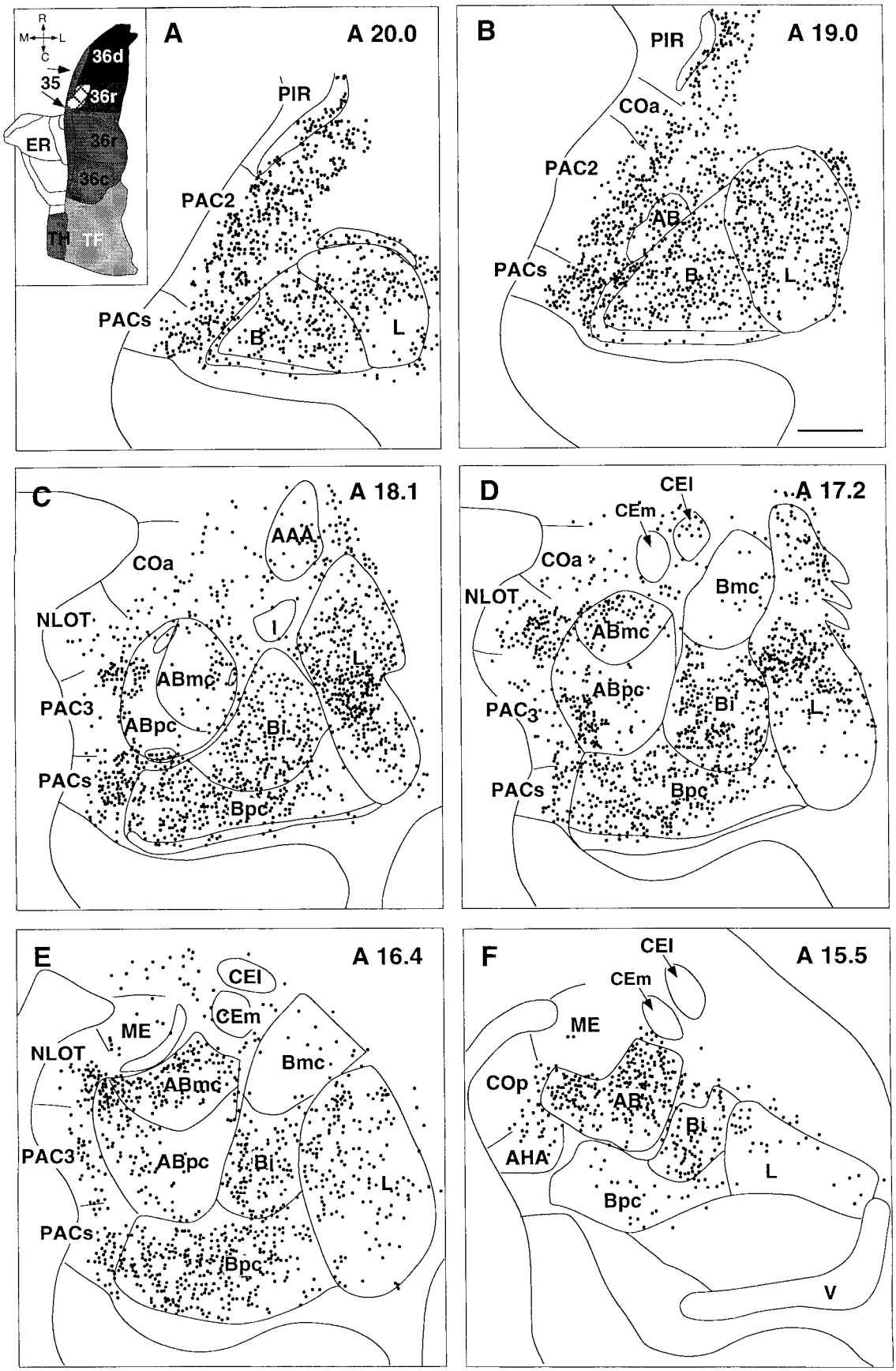


Fig. 14. Line drawings through six levels of the amygdala, arranged from rostral (**A**) to caudal (**F**), that show the distribution of retrogradely labeled cells after the retrograde tracer Fast blue was placed in the polar portion of area 36r (experiment M21-91 FB). This region of the perirhinal cortex was the main target of projections arising from the intermediate and parvicellular divisions of the basal nucleus. V, ventral; R, rostral; C, caudal; M, medial; L, lateral. Scale bar = 1.0 mm and applies to A–F.

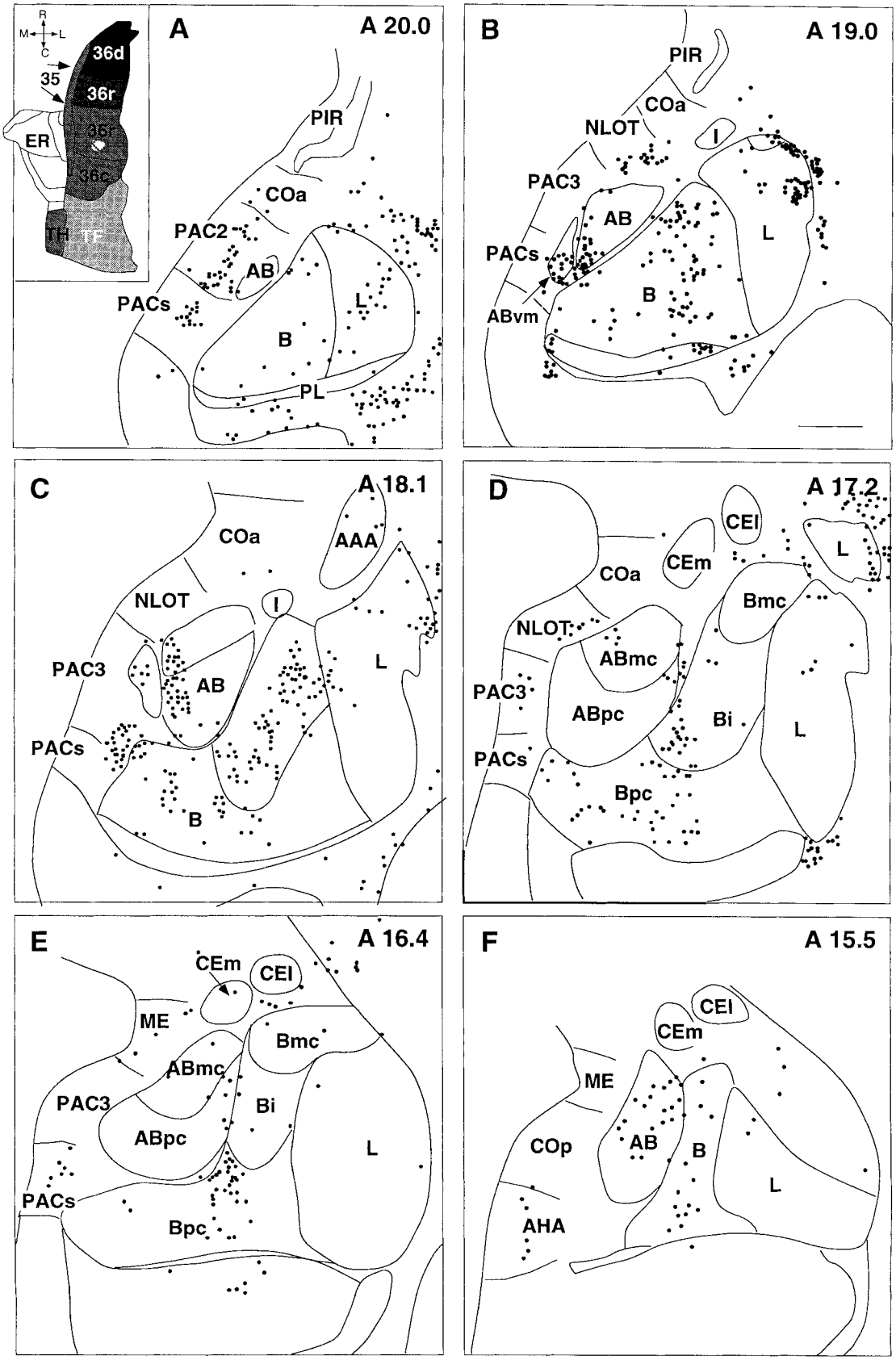


Fig. 15. Line drawings through six levels of the amygdala, arranged from rostral (**A**) to caudal (**F**), that show the distribution of retrogradely labeled cells after the retrograde tracer Fast blue was placed in the ventral portion of area 36r (experiment M3-90 FB). Compared with the density of input directed to the polar regions of the perirhinal cortex, more ventrally directed projections were considerably less robust. R, rostral; C, caudal; M, medial; L, lateral. Scale bar = 1.0 mm and applies to A–F.

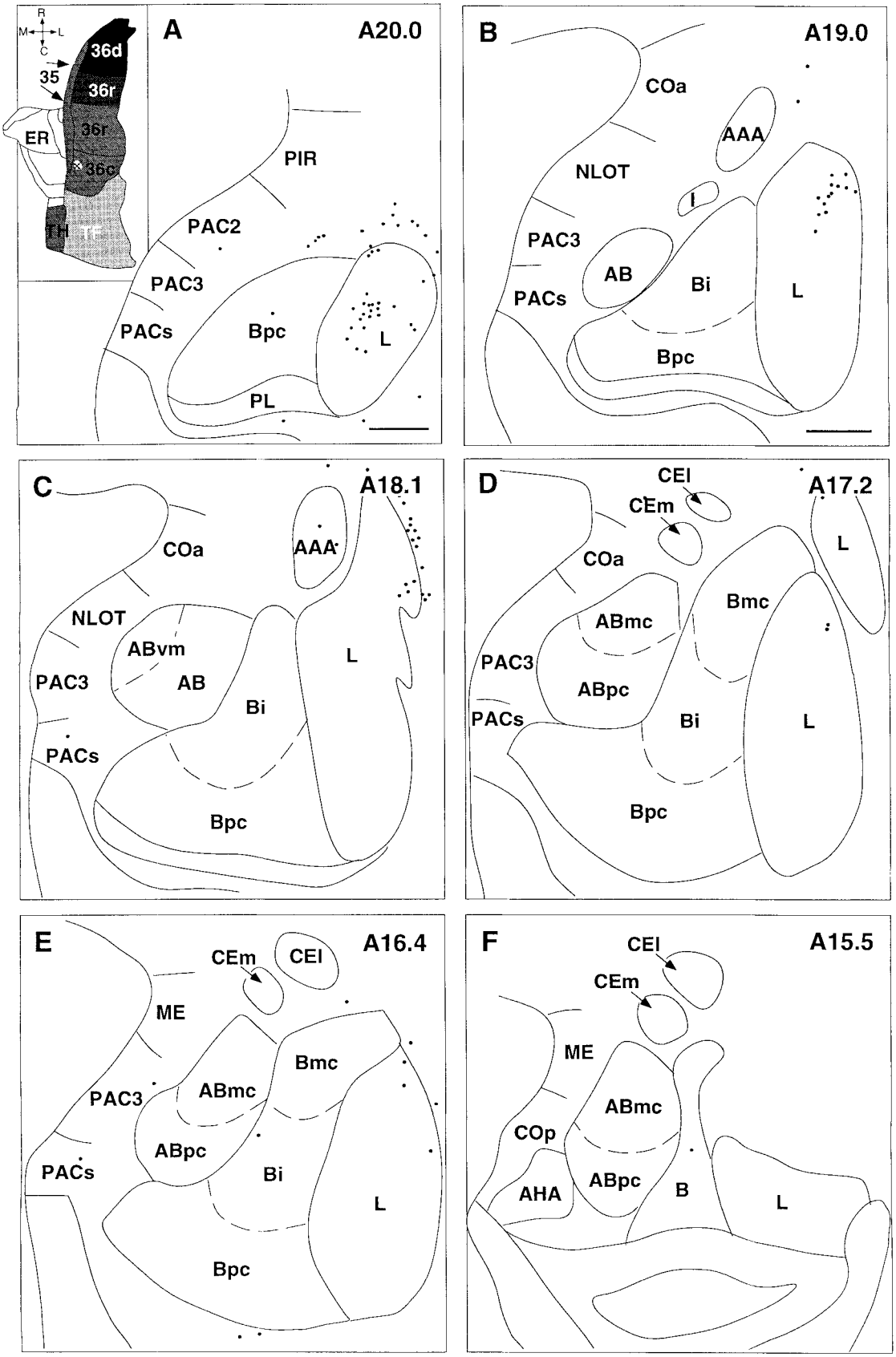


Fig. 16. Line drawings through six levels of the amygdala, arranged from rostral (**A**) to caudal (**F**), that show the distribution of retrogradely labeled cells after the tracer Diamidino yellow was placed in area 36c of the perirhinal cortex (experiment M12-90 DY). Projections to ventral aspects of the perirhinal cortex were generally weak, and this figure demonstrates that they were particularly meager to caudal regions of the cortex. R, rostral; C, caudal; M, medial; L, lateral. Scale bars = 1.0 mm and apply to A–F.

cells counted in the lateral nucleus was only 169 and 57, respectively. The differences in absolute numbers of total retrogradely labeled cells across experiments may reflect different tracer volume or uptake efficiency rather than regional topography. However, evidence from complementary anterograde studies clearly supports the notion of regional variation in amygdala-perirhinal projections (see below).

Projections to area 35 generally respected the rostrocaudal gradient described above. The one exception was the projection from the basal nucleus, which appeared to give rise to a moderate-to-heavy projection to all rostrocaudal levels of area 35. In experiment M4-91 (Fig. 3), an area 35 injection was situated rostrocaudally between an injection of area 36r (Fig. 15) and area 36c (Fig. 16). In this case, projections from most nuclei were weaker than those to area 36r and stronger than those to area 36c. However, projections from the magnocellular, parvicellular, and intermediate divisions of the basal nucleus were greater after the area 35 injection than after those involving either area 36r or 36c.

The anterograde tracing studies confirm our observations of a rostrocaudal gradient in the amygdala projection to the perirhinal cortex. The strong projection to the polar regions of the perirhinal cortex is illustrated in Figure 18. When PHA-L injections were placed in different divisions of the lateral nucleus, a dense and specific plexus of labeled fibers and terminals was observed in the polar portion of area 36r (Fig. 18A) or in area 36d (Fig. 18B). Other amygdaloid nuclei also demonstrated robust projections to rostral regions of the perirhinal cortex. In experiments FCP2 and FCP4, the tritiated amino acid injections included mainly the accessory basal nucleus and the medial aspect of the basal nucleus. In both experiments, heavy anterograde transport was observed in the temporal polar region of the perirhinal cortex. In experiment DM-29R, tritiated amino acids were placed in the anterior cortical nucleus, the nucleus of the lateral olfactory tract and the dorsal medial tip of the accessory basal nucleus. In experiment DM-34L, the injection was more ventrally placed and included the periamygdaloid complex and the most medial aspects of the parvicellular divisions of the basal and accessory basal nuclei. Both experiments resulted in anterograde transport to the polar regions of the perirhinal cortex, although in DM-34L, labeling was generally more robust.

The results of both the retrograde and anterograde studies indicated that the strength of amygdala input to the perirhinal cortex decreased substantially and in a graded fashion at more caudal and ventral regions of the perirhinal cortex. For example, the lateral nucleus projected strongly to the polar portion of the perirhinal cortex and demonstrated additional, weaker projections to more ventrally situated regions of area 36r. There were few, if any, projections directed to caudal regions of area 36. Other nuclei also demonstrated a decreasing gradient of projections to area 36. For example, in experiment FCP4 a large amino acid injection placed in the basal and accessory basal nuclei resulted in heavy anterograde labeling in the rostral polar region of the perirhinal cortex (Fig. 17A). At progressively more caudal levels of area 36, the anterograde labeling became weaker (Fig. 17B–D).

***Topography of amygdala projections to the perirhinal cortex: inter- and intranuclear differences.*** In addition to the overall greater projection of the amygdala to polar levels of the perirhinal cortex, our quantitative analyses indicated that the proportions of cells in each of the amygdaloid nuclei also varied depending on the rostrocaudal location of the perirhinal injection site (Table 1A). For example, when the injection was located in area 36d or 36c, the highest proportions of retrogradely labeled cells were located in the lateral nucleus (62.4% and 74%, respectively), whereas lower proportions were located in the basal nucleus (12.5% and 10.4%, respectively) (Table 1A; Figs. 13, 16). At polar and ventral levels of area 36r, however, there was a shift such that the basal nucleus contributed the highest proportions of total input and the lateral nucleus contributed more modest inputs (Table 1A; Figs. 14, 15).

Within the basal nucleus itself, there were differential projections to the perirhinal cortex. In particular, the magnocellular division of the basal nucleus was distinct in its meager input to the perirhinal cortex, whereas the intermediate and parvicellular divisions originated much more prominent projections (Figs. 13–15). When a retrograde tracer was placed in the polar portion of area 36r, only 0.5% of the input originated from the magnocellular division and 20.9% and 16.4% originated from the parvicellular and intermediate divisions, respectively (Table 1A). The results of anterograde studies confirm this finding: No anterograde transport was observed in the perirhinal cortex after an anterograde tracer was placed in the magnocellular division of the basal nucleus (DM-28L).

The parvicellular division of the basal nucleus also demonstrated subregional differences in its projection to the perirhinal cortex. The caudal pole of the parvicellular division of the basal nucleus originated only weak projections to the perirhinal cortex compared with the more robust input that arose from rostral levels. In our series of retrograde tracer experiments, dyes were placed at several different rostrocaudal levels of the perirhinal cortex. In all cases, only small numbers of retrogradely labeled cells were counted in the caudal pole of the parvicellular division (e.g., Figs. 13F, 14F). Similarly, when an anterograde tracer injection was placed in the caudal pole of the parvicellular division (M8-88), there was only a minor projection to the perirhinal cortex.

***Laminar organization of terminal fields in the perirhinal cortex.*** Inputs from the amygdaloid complex to the perirhinal cortex were directed primarily to layers I/II but also innervated layers V/VI. Interestingly, there appeared to be rostrocaudal differences in the laminar distribution of amygdala inputs to the perirhinal cortex. Amygdala projections were directed to layers I/II and V/VI of rostral perirhinal regions (Fig. 17A,B) but were directed predominantly to layers V/VI (Fig. 17C,D) at caudal levels.

## Organization of connections between the parahippocampal cortex and the amygdaloid complex

***Projections from the parahippocampal cortex to the amygdala: A summary of anterograde and retrograde data.*** In general, the parahippocampal cortex gave rise to only modest projections to the amygdala, and most of these came from area TF. Projections originating in area TF were organized along a rostrocaudal gradient. Within the amygdala, the heaviest projections were to the basal nucleus, particularly to the lateral aspect of its parvicellular division. Weaker projections were directed to the lateral nucleus, and very minor projections went to other nuclei. This pattern is distinct from the perirhinal projections that more heavily innervated the lateral nucleus. We discuss these findings and some relevant experiments below.

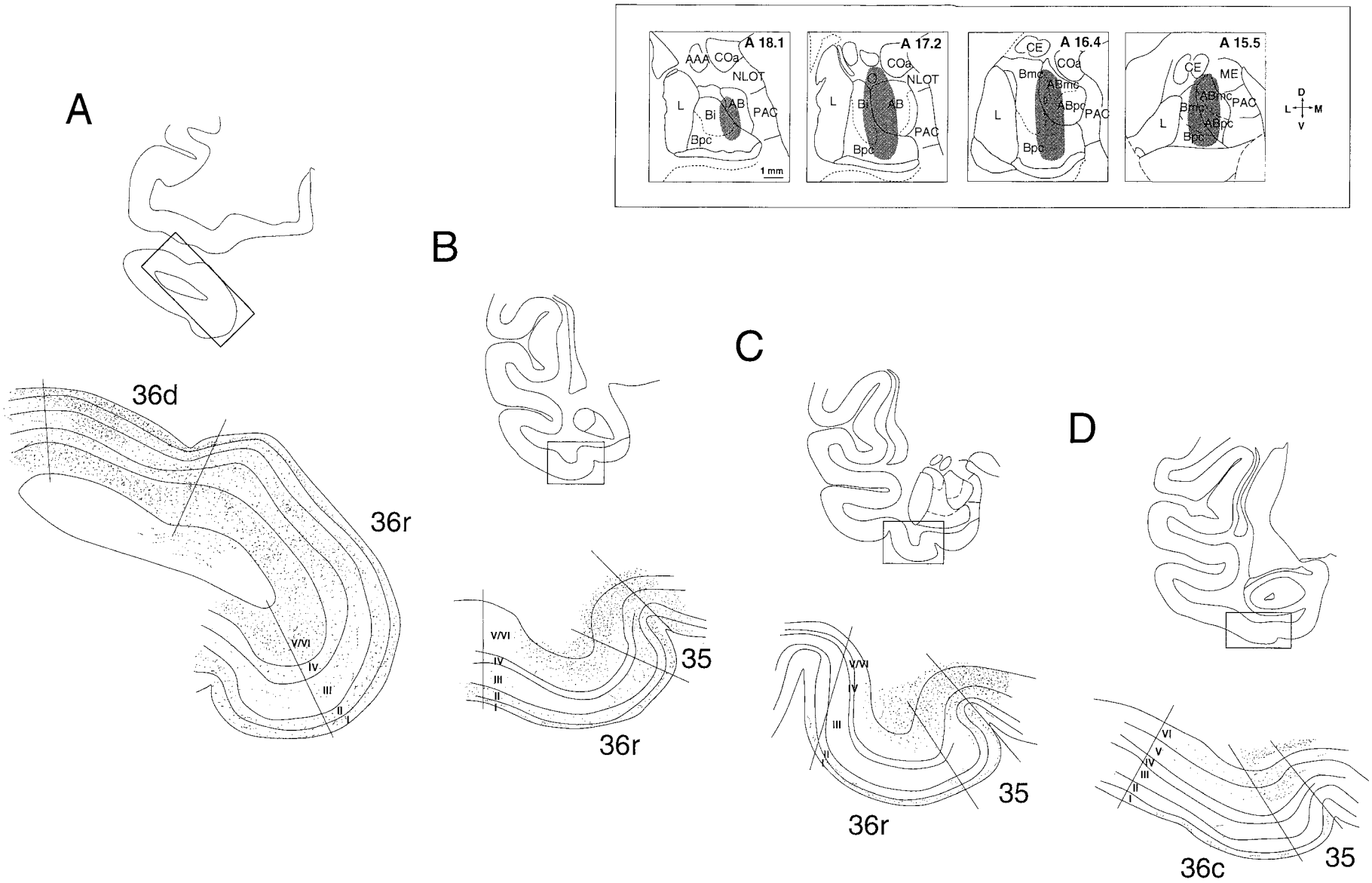


Fig. 17. Line drawings through four levels of the perirhinal cortex from rostral (**A**) to caudal (**D**) that show the laminar distribution of anterogradely transported label after a large injection of $^{3}$H-amino acids was placed in the amygdala. Box at upper right shows the location of the injection site at four rostrocaudal levels of the amygdala. D, dorsal, V, ventral, M, medial, L (experiment FCP4), lateral. Scale bar = 1.0 mm.

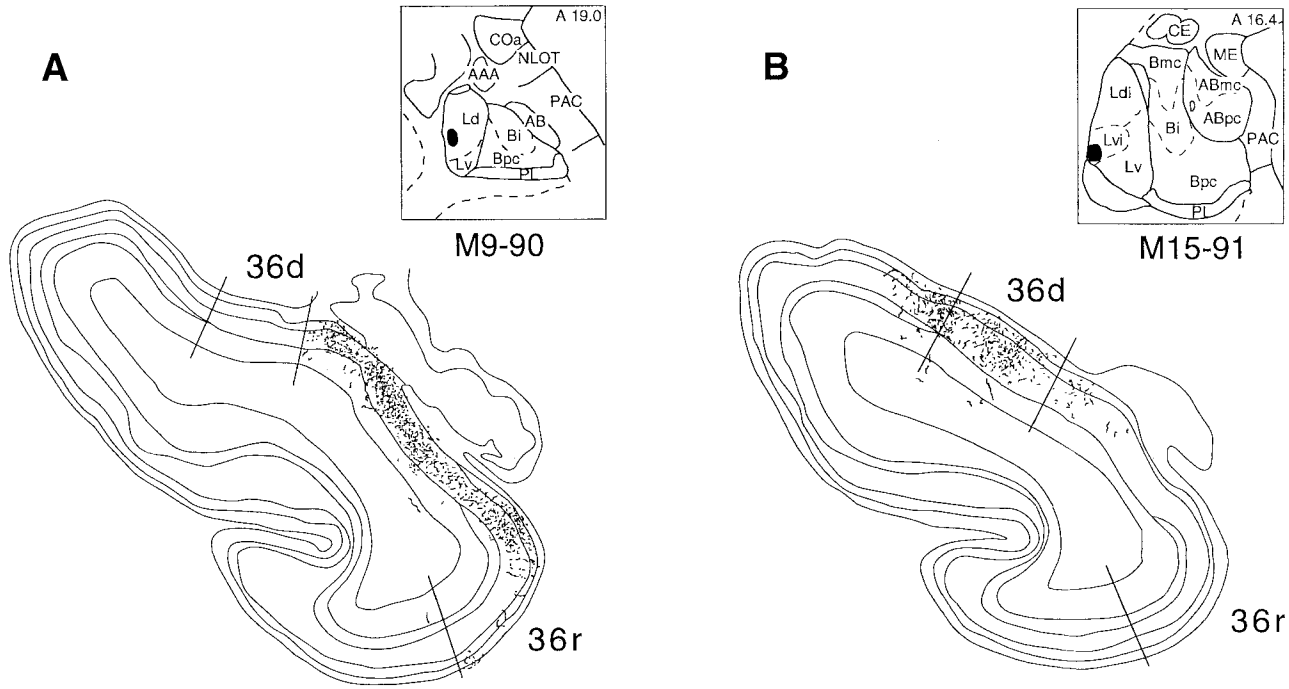


Fig. 18. Distribution of anterogradely transported PHA-L-labeled fibers in the temporal polar portions of area 36 after injections were placed in rostral (**A**) and caudal (**B**) regions of the lateral nucleus. Box to the right of each figure shows a line drawing of a coronal section through the amygdaloid complex, at the level of the injection site.

TABLE 1. Percentage of labeled cells in the different amygdaloid nuclei after retrograde tracer injections were placed in different portions of **A,** the perirhinal cortex, and **B,** the parahippocampal cortex[1]

| Experiment | Vol (nl) | L | Bmc | Bpc | Bi | AB | CE | COa | AAA | NLOT | PAC | ME | COp | AHA | Total cells |
|---|---|---|---|---|---|---|---|---|---|---|---|---|---|---|---|
| A. Percentage labeled cells in the amygdaloid nuclei after retrograde tracers were placed at different levels of the perirhinal cortex | | | | | | | | | | | | | | | |
| M21-91 DY (36d) | 1,000 | 62.4 | 0.9 | 8.5 | 3.1 | 4.3 | 0.0 | 1.9 | 1.1 | 0.5 | 6.0 | 0.7 | 0.5 | 0.1 | 6,276 |
| M21-91 FB (polar 36r) | 600 | 25.4 | 0.5 | 20.9 | 16.4 | 8.7 | 0.2 | 1.7 | 0.6 | 2.2 | 12.0 | 0.2 | 0.5 | 0.7 | 8,576 |
| M3-90 FB (36r) | 500 | 18.0 | 2.0 | 21.0 | 22.3 | 20.9 | 0.1 | 0.6 | 0.5 | 1.5 | 12.1 | 0.5 | 0.0 | 0.4 | 939 |
| M12-90 DY (36c) | 500 | 74.0 | 0.0 | 1.3 | 9.1 | 5.2 | 0.0 | 0.0 | 2.6 | 0.0 | 7.8 | 0.0 | 0.0 | 0.0 | 77 |
| M4-91 FB (area 35) | 500 | 7.4 | 3.9 | 37.9 | 5.8 | 5.2 | 0.0 | 0.5 | 2.2 | 1.0 | 6.0 | 0.0 | 0.0 | 0.1 | 1,150 |
| B. Percentage labeled cells in the amygdaloid nuclei after retrograde tracers were placed at different levels of the parahippocampal cortex | | | | | | | | | | | | | | | |
| M10-90 DY (rostral TF) | 500 | 1.2 | 13.3 | 41.6 | 23.5 | 8.4 | 0.0 | 0.0 | 1.8 | 0.0 | 9.6 | 0.0 | 0.6 | 0.0 | 166 |
| M10-90 FB (middle TF) | 650 | 2.3 | 58.2 | 17.7 | 19.1 | 1.4 | 0.0 | 0.0 | 0.0 | 0.0 | 1.4 | 0.0 | 0.0 | 0.0 | 220 |
| M2-90 FB (caudal TF) | 500 | 2.4 | 83.3 | 1.0 | 12.4 | 0.0 | 0.0 | 0.0 | 0.5 | 0.0 | 0.5 | 0.0 | 0.0 | 0.0 | 210 |
| M15-91 DY (TH) | 1,500 | 34.8 | 4.4 | 8.7 | 0.0 | 13.0 | 0.0 | 0.0 | 30.4 | 0.0 | 8.7 | 0.0 | 0.0 | 0.0 | 23 |

[1] Suffix FB or DY after each experiment indicates the type of retrograde tracer (FB, Fast blue; DY, Diamidino yellow) that was used. The volume (Vol) of retrograde tracer is also indicated for each experiment, as well as the total numbers of retrogradely labeled cells counted in the amygdala for each experiment.

Area TF projected to all divisions of the basal nucleus. However, the strongest projections were directed to the lateral aspect of the parvicellular division. Figure 8 illustrates the anterograde transport in the amygdaloid complex for experiment M13-91, in which a tritiated amino acid injection was placed at a rostral level of area TF (Fig. 3). At all rostrocaudal levels, labeled fibers and terminals were found predominantly in the basal nucleus. There were additional, weaker projections to the lateral, accessory basal, and central nuclei and to the anterior amygdaloid area, but no other amygdaloid region received appreciable input. Projections arising from progressively more caudal levels of the parahippocampal cortex were progressively weaker, although the overall distribution of anterograde label was the same.

Our results suggest that area TH may also contribute a minor projection to the amygdala. In experiment M4-94, an anterograde tracer injection was placed in the rostral portion of area TH and also involved a small part of the caudal limiting division of the entorhinal cortex. In this case, there was a moderate plexus of labeled fibers and terminals in the parvicellular division of the basal nucleus. The plexus was situated laterally and was only present in the caudal half of the amygdala. A few labeled fibers were observed in the medial aspect of the parvicellular division of the basal nucleus, and even fewer were seen in the lateral nucleus.

The results of our retrograde tracing experiments confirmed the presence of meager projections from the parahippocampal cortex to the lateral and accessory basal nuclei. Figure 11A–D show the distribution of parahippocampal input to different divisions of the lateral nucleus. There were consistently low numbers of retrogradely labeled cells in areas TF and TH. There were similarly low numbers of retrogradely labeled cells in the parahippocampal cortex

after injections into the magnocellular and parvicellular divisions of the accessory basal nucleus (Figure 11E,F).

***Laminar distribution of parahippocampal input to the amygdala.*** Most of the input from areas TF and TH to the amygdala arose from layers V/VI. This can be seen on the unfolded map in Figure 12, where we show the laminar distribution of cortical input to the lateral nucleus. Most retrogradely labeled cells (76–100%) were identified in the infragranular layers.

***Projections from the amygdala to the parahippocampal cortex.*** The projections from the amygdala to the parahippocampal cortex were also modest and could be characterized by three major features. First, most input was directed to area TF. Second, the projections to area TF originated predominantly in the magnocellular division of the basal nucleus. Weaker projections arose from other subdivisions of the basal nucleus and to a lesser degree from the lateral and accessory basal nuclei, as well as from the periamygdaloid cortex and the anterior amygdaloid area. Finally, the proportions of projecting cells in different divisions of the basal nucleus varied depending on the rostrocaudal level of area TF that received the retrograde tracer injection. Thus, the magnocellular division of the basal nucleus gave rise to a proportionately greater projection to caudal levels of area TF than to rostral levels, whereas other divisions of the basal nucleus demonstrated an inverse projection pattern.

The most significant input from the amygdala to the parahippocampal cortex arose from the magnocellular division of the basal nucleus. Figure 19 shows the distribution of retrograde label in the amygdala for an experiment in which a retrograde tracer was placed in area TF (Fig. 3B). Retrogradely labeled cells were located almost exclusively in the magnocellular division of the basal nucleus, (Fig. 19D,E), although scattered cells were also observed in the intermediate division of the basal nucleus and an occasional cell was identified in the lateral nucleus, the anterior amygdaloid area, and the periamygdaloid cortex.

The magnocellular division of the basal nucleus contributed progressively denser projections to progressively more caudal regions of area TF. Table 1B shows the numerical data for four experiments in which retrograde tracers were placed at different levels of the parahippocampal cortex. The magnocellular division of the basal nucleus contributed only 13.3% of the total amygdaloid input to rostral levels of area TF (M10-90 DY), whereas it contributed 58.2% and 83.3% to mid rostrocaudal and caudal levels, respectively (M10-90 FB and M2-90 FB).

In contrast to the *increasing* projection gradient from the magnocellular division of the basal nucleus, the intermediate and parvicellular divisions of the basal nucleus demonstrated progressively *decreasing* projections to successively more caudal levels of area TF (Table 1B). The parvicellular division of the basal nucleus contributed 41.6%, 17.7%, and 1.0% of total amygdala input to rostral, mid-rostrocaudal and caudal regions of area TF, respectively. Similarly, the intermediate division of the basal nucleus contributed 23.5%, 19.1%, and 12.4% input to progressively more caudal levels of area TF. More subtle decreasing gradients were also observed for projections from some of the other amygdaloid nuclei, such as the accessory basal nucleus, the anterior amygdaloid area, and the periamygdaloid cortex (Table 1B).

The results of retrograde tracing experiments indicated that the amygdala originates only a scant projection to area TH. When a retrograde tracer was placed in area TH (M15-91 DY, Fig. 3), only a few retrogradely labeled cells were observed in the amygdala (Table 1B). These were located in the deep nuclei, the anterior amygdaloid area, and the periamygdaloid cortex.

The results of anterograde tracing studies corroborated the findings from the retrograde tracing experiments discussed above. Large injections of anterograde tracer that included the parvicellular and intermediate divisions of the basal nucleus, the accessory basal nucleus, and the periamygdaloid cortex (e.g., FCP-4) resulted in weak anterograde transport primarily to rostral regions of the parahippocampal cortex. A more discrete injection of the parvicellular division of the basal nucleus similarly resulted in light transport only to rostral regions of the parahippocampal cortex. Notably, labeled fibers and terminals were observed both in areas TF and TH, although the projection to area TF was more prominent. In an experiment in which the deposit of anterograde tracer heavily involved the magnocellular division of the basal nucleus, by contrast, scattered fibers and terminals were observed only in caudal regions of areas TF and TH. In the lateral nucleus, the dorsal intermediate division gave rise only to scattered fibers in the superficial layers of areas TF and TH.

***Laminar distribution of amygdala input to the parahippocampal cortex.*** The terminal fields of amygdala projections in the parahippocampal cortex were confined mostly to the superficial cortical layers. These findings are based on experiments originally described by Amaral and Price (1984) and are more fully discussed in their report.

## DISCUSSION

The PRPH cortices have been linked, both anatomically and functionally, to the hippocampal formation and to the mediation of normal memory (Insausti et al., 1987; Zola-Morgan et al., 1989; Meunier et al., 1993; Suzuki et al., 1993; Eacott et al., 1994; Suzuki and Amaral, 1994a,b). Several previous studies have also demonstrated substantial interconnections between the amygdala and at least the temporal polar portion of the perirhinal cortex (Aggleton et al., 1980; Moran et al., 1987). Yet, the precise topography of these connections and the relationship of the amygdala with more caudal regions of the perirhinal cortex and with the parahippocampal cortex have not been comprehensively described. Thus, the goal of this study was to clarify the organization of connections between the amygdaloid complex and the PRPH cortices and, in particular, to compare the magnitude and topography of these connections with those involving the hippocampal formation.

### Summary of results

The present results both confirm and extend previous findings. Perhaps the major contribution of the present study is the description of the topographic organization of reciprocal connections between specific amygdaloid nuclei and cytoarchitectonically distinct regions of the PRPH cortices.

The amygdaloid complex has prominent and widespread connections with the perirhinal cortex and weaker and more restricted connections with the parahippocampal cortex. The densest projections to the amygdala arose from temporal polar levels of the perirhinal cortex and less prominent projections arose from more ventrocaudal levels (Fig. 20). Perirhinal projections terminated mainly in the dorsal divisions of the lateral nucleus, the lateral portion of the parvicellular division of the basal nucleus, the magnocellular division of the basal nucleus, and the magnocellular division of the accessory basal nucleus. Weaker projections

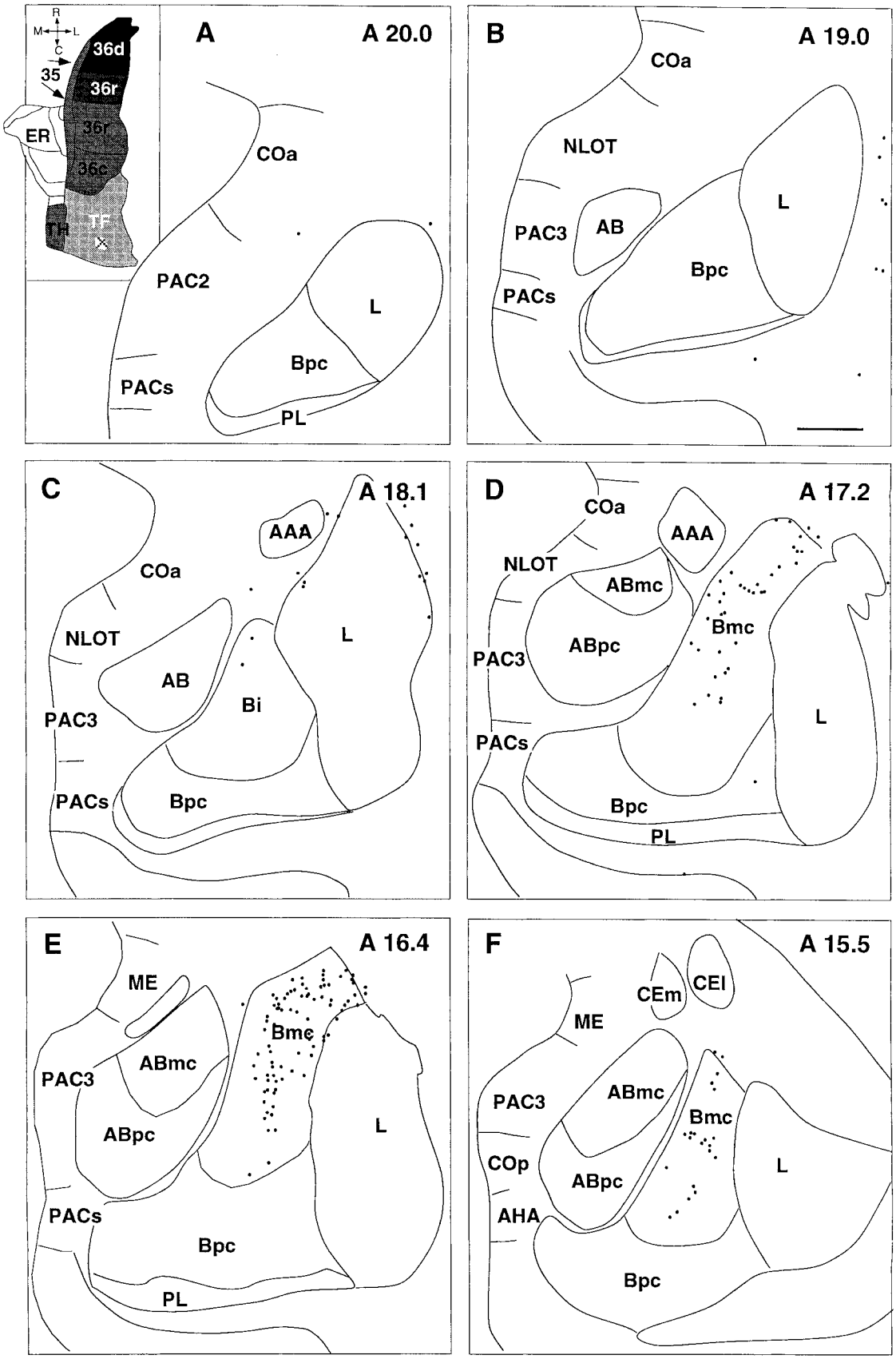


Fig. 19. Line drawings through six levels of the amygdala, arranged from rostral (**A**) to caudal (**F**), that show *the distribution of* retrogradely labeled cells after the retrograde tracer Fast blue was placed in area TF of the parahippocampal cortex (experiment M2-90 FB). Input arose predominantly from the magnocellular division of the basal nucleus (D–F). R, rostral; C, caudal; M, medial; L, lateral. Scale bar = 1.0 mm and applies to A–F.

terminated in the periamygdaloid cortex, the anterior and posterior cortical nuclei, the medial nucleus, and the anterior amygdaloid area. There was some evidence for a weak projection from the perirhinal cortex to the central nucleus. Projections arose both from areas 35 and 36 but were somewhat stronger from area 36.

The amygdala contributed dense return projections to polar levels of the perirhinal cortex and weaker projections to more caudal levels. Projections to rostral perirhinal regions arose mainly from the lateral, basal, and accessory basal nuclei and the periamygdaloid cortex, whereas projections to caudal perirhinal levels arose only from the lateral nucleus. The intermediate and parvicellular divisions of the basal nucleus projected throughout the rostrocaudal extent of area 35, with somewhat lighter projections to more caudal levels. The magnocellular division of the basal nucleus did not appear to project to any portion of the perirhinal cortex.

Parahippocampal input to the amygdala arose mostly from area TF. Rostral levels of area TF projected more heavily to the amygdala, and these projections terminated in the lateral portion of the parvicellular division of the basal nucleus. Weaker inputs from rostral area TF were directed to the other divisions of the basal nucleus, the lateral nucleus, and to more medially situated nuclei. Caudal area TF gave rise to only meager projections to the amygdala, although the distribution of these projections was similar to those originating rostrally. Projections from the amygdala to the parahippocampal cortex were also directed mainly to area TF. Interestingly, unlike the projections to the perirhinal cortex, these projections originated principally in the magnocellular division of the basal nucleus. These projections were more prominent to caudal levels of TF than to rostral levels. In this regard, the amygdala's projections to caudal area TF resembled its projections to the visual areas TE and TEO (Iwai and Yukie, 1987), which also receive amygdaloid input mainly from the magnocellular division of the basal nucleus. Input from the intermediate and parvicellular divisions of the basal nucleus to area TF was weaker and was directed mainly to rostral levels of the parahippocampal cortex.

## Comparison with previous studies

***Projections from the perirhinal cortex to the amygdala.*** Our finding of a robust rostral perirhinal (temporal polar) input to the amygdala confirms earlier findings by Aggleton et al. (1980). They concluded that the temporal pole projected heavily to the lateral and accessory basal nuclei and more weakly to the magnocellular and intermediate divisions of the basal nucleus. They also found that caudoventral portions of the perirhinal cortex projected mainly to the basal nucleus. These results are consistent with our own findings. Iwai and Yukie (1987) placed injections of horseradish peroxidase into different portions of the inferotemporal cortex and surveyed the distribution of anterogradely labeled terminals in the amygdaloid complex. Injections confined to area TE resulted in a limited distribution of anterogradely transported label within the amygdala, particularly within the dorsal aspect of the lateral nucleus. By contrast, ventrally situated injections that involved the perirhinal cortex gave rise to more substantial and widely distributed projections to the lateral, basal, and accessory basal amygdaloid nuclei. Similarly, Herzog and Van Hoesen (1976) noted that only when lesions of area TE included portions of area 35 was there anterograde degeneration within the parvicellular division of the basal nucleus. Van Hoesen (1981) reported that discrete injections of tritiated amino acids into area 35 resulted in anterograde transport to the parvicellular divisions of the basal and accessory basal nuclei.

***Projections from the amygdala to the perirhinal cortex.*** Our findings of robust and widespread projections from the amygdaloid complex to the polar portion of the perirhinal cortex confirms findings by Moran et al. (1987), who identified retrogradely labeled neurons in most of the amygdaloid nuclei after placing tracer injections into rostral perirhinal regions (see also Markowitsch et al., 1985).

Previous studies have also provided evidence that the amygdala projects to caudoventral levels of the perirhinal cortex (Iwai and Yukie, 1987; Saunders and Rosene, 1988). Consistent with our findings, Iwai and Yukie (1987) noted retrogradely labeled cells in the parvicellular division of the basal nucleus and in the lateral and accessory basal nuclei after a retrograde tracer injection that involved a ventral level of the perirhinal cortex (see also Saunders and Rosene, 1988; Amaral and Price, 1984).

***Projections from the parahippocampal cortex to the amygdala.*** Herzog and Van Hoesen (1976) did not find evidence of amygdaloid projections arising from the parahippocampal cortex. This is in contrast to our findings, which indicate that although the posterior parahippocampal cortex may not generate a projection to the amygdala, the rostral parahippocampal cortex certainly does. The greater sensitivity of the autoradiographic tracing method used in the present study as compared with the silver degeneration technique used by Herzog and Van Hoesen may account for this discrepancy. Consistent with this idea are data presented in the brief report by Van Hoesen (1981) based on studies using the autoradiographic tracing method in support of parahippocampal-amygdaloid projections. These projections were reported to be directed to the central nucleus and to the magnocellular division of the basal nucleus. Our findings are not entirely consistent with those reported by Van Hoesen (1981) because we observed only very light projections from the parahippocampal cortex to the central nucleus, for example. Moreover, although we observed projections to the magnocellular division of the basal nucleus, more prominent projections were observed to the parvicellular division of the basal nucleus as well as to the lateral and accessory basal nuclei. These latter projections were not reported by Van Hoesen (1981).

Aggleton et al. (1980) reported that injections of retrograde tracers centered in the lateral nucleus resulted in a few retrogradely labeled cells in areas TF and TH. This finding is consistent with the weak projections that we observed from the parahippocampal cortex to the lateral nucleus. Interestingly, Aggleton et al. (1980) did not report the robust projection from the parahippocampal cortex to the basal nucleus that we observed. This is particularly surprising because several of their large HRP injections involved the basal nucleus.

***Projections from the amygdala to the parahippocampal cortex.*** We are aware of only one study that reported projections from the amygdala to the parahippocampal cortex in the monkey (Amaral and Price, 1984). The data from this study have been summarized in the Results section.

## Comparison of amygdala-perirhinal connections with amygdala-parahippocampal connections

We have emphasized that the connections between the amygdala and the perirhinal cortex (particularly the polar

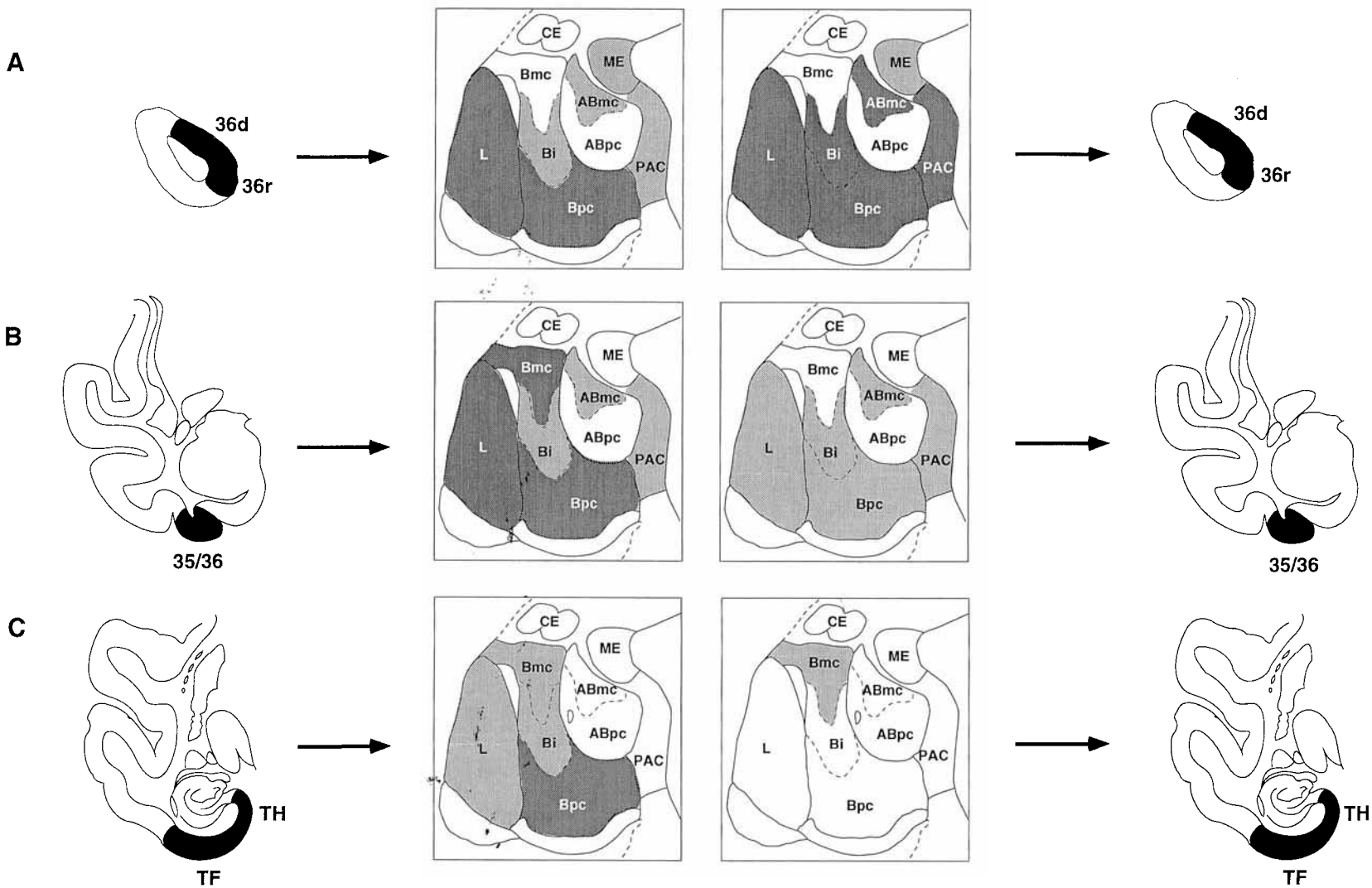


Fig. 20. Summary of interconnections between the perirhinal and parahippocampal (PRPH) cortices and the amygdala. The subdivisions of the PRPH cortices are indicated in black on the temporal lobe icons. The gray levels in different amygdaloid nuclei represent the density of the projections *from* (left half of figure) or *to* (right half of figure) the PRPH cortices. Dark gray, heavy to moderate; light gray, moderate to light. The anterior and posterior cortical nuclei, anterior amygdaloid nucleus, and the nucleus of the lateral olfactory tract are also weakly interconnected with the perirhinal cortex (temporal polar region) but are not represented on this figure. See text for connectional distinctions among different subdivisions of the lateral nucleus and between medial versus lateral portions of the parvicellular division of the basal nucleus.

portion of the perirhinal cortex) were different from those with the parahippocampal cortex. Input from the perirhinal cortex was more robust than input from the parahippocampal cortex and had a more distributed termination pattern. Return projections to the PRPH cortices were also different. Projections from the amygdala to the perirhinal cortex arose from distributed regions of the amygdala but notably not from the magnocellular division of the basal nucleus. This pattern is similar to its projections to "limbic" structures such as the hippocampal formation and the orbitofrontal cortex (Porrino et al., 1981; Amaral and Price, 1984; Amaral, 1986; Saunders et al., 1988; Barbas and De Olmos, 1990). By contrast, projections to the parahippocampal cortex were weaker and arose almost exclusively from the magnocellular division of the basal nucleus. This projection pattern resembles amygdaloid projections to sensory cortical regions (Tigges et al., 1982; Amaral and Price, 1984; Iwai and Yukie, 1987).

The question arises as to the functional significance of these differential projection patterns. One hint may come from the types of information that enter the PRPH cortices. The PRPH cortices receive distinctly different complements of cortical inputs (Suzuki and Amaral, 1994a). The perirhinal cortex receives prominent inputs from unimodal visual areas TE and TEO. Areas TE and TEO, in turn, are associated with the "ventral stream" cortical pathway that processes primarily visual object information (Ungerleider and Mishkin, 1982; Van Essen and Maunsell, 1983). Although the TE/TEO input would seem to be a dominant influence on perirhinal function, the perirhinal cortex also receives inputs from polysensory regions, the most prominent of which is the parahippocampal cortex. The parahippocampal cortex also receives visual input but from different cortical regions (e.g., area V4) than those that project to the perirhinal cortex. Additionally, in contrast to the perirhinal cortex, the parahippocampal cortex receives major inputs from the retrosplenial cortex, the dorsal bank of the superior temporal sulcus, and the posterior parietal cortex.

Because the PRPH cortices have been implicated in the mediation of normal memory (Zola-Morgan et al., 1989; Meunier et al., 1993; Suzuki et al., 1993; Eacott et al., 1994), the differences in connectional patterns described above have prompted the speculation that the perirhinal cortex may be particularly involved in visual object recognition memory whereas the parahippocampal cortex may subserve visuospatial memory (Suzuki and Amaral, 1994a; see also Nakamura et al., 1994). Returning to the amygdala, it would appear that the predominance of interconnections with the perirhinal cortex over those with parahippocampal cortex would indicate that the amygdala is more highly influenced by information about the physical appearance of objects rather than their location or movement in space. This is not to say that there are no routes for motion or spatial information to reach the amygdala, because the weaker connections between the parahippocampal cortex and the amygdala or the parahippocampal connections with the perirhinal cortex do provide indirect routes for this information to reach the amygdala. These indirect routes may take on added functional significance because there appear to be no direct projections from the parietal cortex (i.e., the "dorsal visual stream") (Ungerleider and Mishkin, 1982; Van Essen and Maunsell, 1983) to the amygdala (Aggleton et al., 1980; Stefanacci and Amaral, 1993; unpublished observations). Only the superior temporal polysensory area, which contains high-order motion and spatial-sensitive neurons (Bruce et al., 1981), has direct connections with the amygdala (Aggleton et al., 1980; Stefanacci and Amaral, 1993; unpublished observations). If the amygdala is, in fact, influential in determining the affective significance of stimuli that an animal experiences, one might presume that not only the size and shape of an object but also whether the object is moving toward or away from the animal would be salient characteristics for such a determination.

## Comparison of amygdala-PRPH connections with hippocampal-PRPH connections

One of the motivating questions for these studies was how the topographic organization of PRPH projections to the amygdala compared with the organization we observed earlier (Suzuki and Amaral, 1994b) for the projections with the hippocampal formation, particularly the entorhinal cortex. That is, we were interested in whether the emotion-related functions of the amygdala and the memory-related functions of the hippocampal formation were supported by similar or different cortical interconnections.

Both with the amygdala and with the hippocampal formation, we have observed widespread and reciprocal connections with the PRPH cortices (Insausti et al., 1987; Suzuki and Amaral, 1994b; present study). Thus, it is possible, and even likely, that some perirhinal neurons, particularly those in the temporal polar region, might project to both of these regions. This possibility will need to be directly evaluated in future double retrograde tracer experiments. However, to what extent can we conclude, with existing data, that the PRPH interconnections with the amygdala are qualitatively or quantitatively different from those with the hippocampal formation?

We found both similarities and differences in the organization and strength of PRPH-amygdala and PRPH-entorhinal connections. All regions of the perirhinal cortex originated projections both to the amygdala and to the entorhinal cortex. However, the projection to the amygdala originated predominantly from the polar regions, whereas the projection to the entorhinal cortex originated more uniformly from the rostrocaudal extent of the perirhinal cortex (Aggleton et al., 1980; Turner et al., 1980; Insausti et al., 1987; Suzuki and Amaral, 1994b; present study). Moreover, medial portions of areas 36r and 36c projected more heavily to the entorhinal cortex than did the lateral portions, but the full mediolateral extent of the perirhinal cortex projected with approximately equal magnitude to the amygdala. Regarding return projections, the amygdala innervated primarily rostral regions of the perirhinal cortex (areas 36d and 36r), whereas the entorhinal cortex projected throughout its rostrocaudal extent. In addition, the parahippocampal cortex had strong interconnections with the entorhinal cortex (Suzuki and Amaral, 1994b), whereas the amygdala has much more modest interconnections.

The organization described above indicates that parts of the perirhinal cortex, particularly the rostral, polar region, are at least as strongly related to the amygdala as they are to the hippocampal formation. This finding complements those of Saunders and Rosene (1988) and Saunders et al. (1988), who demonstrated that amygdala and hippocampal inputs to the perirhinal cortex have overlapping distributions.

The parahippocampal cortex, however, has a preferential relationship with the hippocampal formation. This finding suggests that while the rostral perirhinal cortex may be

involved in both affective and memory functions, the parahippocampal cortex may be more strongly involved with hippocampal-dependent memory than with emotion. Future lesion and electrophysiological studies will be needed to test this prediction.

### A special role for the temporal pole in emotional processing?

Our findings of robust and widespread interconnections between the polar portion of the perirhinal cortex and the amygdaloid complex suggest that these two regions may subserve similar functions. There are, in fact, data from lesion studies in monkeys that support this notion. Removal of large portions of the temporal lobe resulted in profound emotional changes in monkeys (Brown and Schafer, 1887; Kluver and Bucy, 1938, 1939; see also Rosvold et al., 1954; Weiskrantz, 1956; Horel et al., 1975) (i.e., the Kluver-Bucy syndrome). The use of stereotaxic lesion techniques demonstrated that circumscribed removal of the amygdaloid complex (Aggleton and Passingham, 1980; Zola-Morgan et al., 1991) was sufficient to produce most components of the Kluver-Bucy syndrome. Although data are more limited, studies with lesions of the temporal polar cortex that spared the amygdala produced a remarkably similar spectrum of changes in social and emotional behavior in monkeys. In animals postoperatively returned to free-ranging conditions, for example, those with temporal polar lesions failed to return to their social group and demonstrated decreased aggressiveness to other monkeys and humans (Myers and Swett, 1970; Kling and Steklis, 1976). Monkeys with these lesions who were maintained in enclosed compounds with their social group were also less aggressive than control animals. The lesioned animals often exhibited hyperorality and lack of fear to normally threatening stimuli. They also demonstrated a decreased tendency to interact with others, as measured by grooming, facial expressions, and vocalizations, and a consequent loss of social status (Franzen and Myers, 1973; Kling and Steklis, 1976; Kling et al., 1993). Animals with similar lesions who were housed singly also exhibited hyperorality, increased exploratory behavior, and decreased emotionality (Horel et al., 1975). Given our current understanding of the important connections of the perirhinal cortex and amygdaloid complex, it would perhaps be worthwhile to re-evaluate the role of selective lesions of the perirhinal cortex or amygdala or conjoint lesions on social interactions in the monkey. The temporal polar portion of the perirhinal cortex not only has strong connections with the amygdala but is also interconnected with orbitofrontal areas (Aggleton et al., 1980; Markowitsch et al., 1985; Moran et al., 1987; Suzuki and Amaral, 1994a) that have themselves been associated with emotional and social behavior (Butter and Snyder, 1971; Teuber, 1972; Franzen and Myers, 1973). Interestingly, the amygdala also has direct and prominent interconnections with much of the orbitofrontal cortex (Aggleton et al., 1980; Porrino et al., 1981; Amaral and Price, 1984; Barbas and De Olmos, 1990; Stefanacci and Amaral, 1993; Carmichael and Price, 1995). Thus, recent neuroanatomical data provides added support for the notion advanced by Kling and colleagues (Kling and Steklis, 1976) that the amygdala, along with the temporal polar (perirhinal) cortex and orbitofrontal cortex, forms an anatomically interconnected network that underlies the mediation of normal social interactions and the orchestration of appropriate species-specific responses. The challenge for future studies is to determine what particular roles are played by the individual members of this emotional triumvirate.

## ACKNOWLEDGMENTS

This work was carried out, in part, at the California Regional Primate Research Center (RR 00169) and was supported by NIH grants R37 MH41479 and NS16980 to D.G.A. and by NIMH predoctoral fellowships MH 10033-02 and MH 10631-01 to W.A.S. and L.S. We thank Janet Weber and Mary Ann Lawrence for excellent histological assistance, and Brian Leonard, Asla Pitkänen, and the staff of the CRPRC for superb surgical assistance.

## LITERATURE CITED

Aggleton, J.P., and R.E. Passingham (1980) Syndrome produced by lesions of the amygdala in monkeys (*Macaca mulatta*). J. Comp. Physiol. Psych. *95*:961–977.

Aggleton, J.P., M.J. Burton, and R.E. Passingham (1980) Cortical and subcortical afferents to the amygdala of the rhesus monkey (*Macaca mulatta*). Brain Res. *190*:347–368.

Amaral, D.G. (1986) Amygdalohippocampal and amygdalocortical projections in the primate brain. In R. Schwarcz and Y. Ben-Ari (eds): Excitatory Amino Acids and Epilepsy. New York: Plenum, pp. 3–17.

Amaral, D.G., and J.L. Bassett (1989) Cholinergic innervation of the monkey amygdala: An immunohistochemical analysis with antisera to choline acetyltransferase. J. Comp. Neurol. *281*:337–361.

Amaral, D.G., and R. Insausti (1992) Retrograde transport of D-($^3$H)-aspartate injected into the monkey amygdaloid complex. Exp. Brain Res. *88*:375–388.

Amaral, D.G., and J.L. Price (1983) An air pressure system for the injection of tracer substances into the brain. J. Neurosci. Methods *9*:35–43.

Amaral, D.G., and J.L. Price (1984) Amygdalo-cortical projections in the monkey (*Macaca fascicularis*). J. Comp. Neurol. *230*:465–496.

Barbas, H., and J. De Olmos (1990) Projections from the amygdala to basoventral and mediodorsal prefrontal regions in the rhesus monkey. J. Comp. Neurol. *300*:549–571.

Brown, S., and E.A. Schafer (1887) An investigation into the functions of the occipital and temporal lobes of the monkey's brain. Philos. Trans. R. Soc. Lond. [Biol] *179B*:303–327.

Bruce, C., R. Desimone, and C.G. Gross (1981) Visual properties of neurons in a polysensory area in superior temporal sulcus of the macaque. J. Neurophysiol. *46*:369–384.

Butter, C.M., and D.R. Snyder (1971) Alterations in aversive and aggressive behaviors following orbital frontal lesions in rhesus monkeys. Acta Neurobiol. Exp. *32*:525–565.

Carmichael, S.T., and J.L. Price (1995) Limbic connections of the orbital and medial prefrontal cortex in macaque monkeys. J. Comp. Neurol. *363*:642–664.

Cowan, W.M., D.I. Gottlieb, A.E. Hendrickson, J.L. Price, and T.A. Woolsey (1972) The autoradiographic demonstration of axonal connections in the central nervous system. Brain Res. *37*:21–51.

Davis, M. (1992) The role of the amygdala in fear and anxiety. Annu. Rev. Neurosci. *15*:353–375.

Desimone, R., and C.G. Gross (1979) Visual areas in the temporal cortex of the macaque. Brain Res. *178*:363–380.

Eacott, M.J., D. Gaffan, and E.A. Murray (1994) Preserved recognition memory for small sets, and impaired stimulus identification for large sets, following rhinal cortex ablations in monkeys. Eur. J. Neurosci. *6*:1466–1478.

Franzen, E.A., and R.E. Myers (1973) Neural control of social behavior: Prefrontal and anterior temporal cortex. Neuropsychologia *1*:141–157.

Gaffan, D., and S. Harrison (1987) Amygdalectomy and disconnection in visual learning for auditory secondary reinforcement by monkeys. J. Neurosci. *7*:2285–2292.

Gallagher, M., and A.A. Chiba (1996) The amygdala and emotion. Curr. Opin. Neurobiol. *6*:221–227.

Herzog, A.G., and G.W. Van Hoesen (1976) Temporal neocortical afferent connections to the amygdala in the rhesus monkey. Brain Res. *115*:57–69.

Horel, J.A., E.G. Keating, and L.J. Misantone (1975) Partial Kluver-Bucy syndrome produced by destroying temporal neocortex or amygdala. Brain Res. *94:*347–359.

Insausti, R., D.G. Amaral, and W.M. Cowan (1987) The entorhinal cortex of the monkey: II. Cortical afferents. J. Comp. Neurol. *264:*356–395.

Iwai, E., and M. Yukie (1987) Amygdalofugal and amygdalopetal connections with modality-specific visual cortical areas in macaques (*Macaca fuscata, M. mulatta,* and *M. fascicularis*). J. Comp. Neurol. *261:*362–387.

Jones, B., and M. Mishkin (1972) Limbic lesions and the problem of stimulus-reinforcement associations. Exp. Neurol. *36:*362–377.

Jones, E.G., and T.P.S. Powell (1970) An anatomical study of converging sensory pathways within the cerebral cortex of the monkey. Brain *93:*793–820.

Kesner, R.P. (1992) Learning and memory in rats with an emphasis on the role of the amygdala. In J.P. Aggleton (ed): The Amygdala: Neurobiological Aspects of Emotion, Memory, and Mental Dysfunction. New York: Wiley-Liss, pp. 379–400.

Kling, A., and H.D. Steklis (1976) A neural substrate for affiliative behavior in nonhuman primates. Brain Behav. Evol. *12:*216–238.

*Kling,* A.S., K. Tachiki, and R. Lloyd (1993) Neurochemical correlates of the Kluver-Bucy syndrome by in vivo microdialysis in monkey. Behav. Brain Res. *56:*161–170.

Kluver, H., and P.C. Bucy (1938) An analysis of certain effects of bilateral temporal lobectomy in the rhesus monkey, with special reference to "psychic blindness." J. Psychol. *5:*33–54.

Kluver, H., and P.C. Bucy (1939) Preliminary analysis of functions of the temporal lobes in monkeys. Arch. Neurol. Psych. *42:*979–997.

LeDoux, J.E. (1987) Emotion. In Handbook of Physiology. The Nervous System V. Washington, D.C.: Amer. Phys. Society, pp. 419–459.

LeDoux, J.E. (1995) Emotion: Clues from the brain. Annu. Rev. Psychol. *46:*209–235.

Markowitsch, H.J., D. Emmans, E. Irle, M. Streicher, and B. Preilowski (1985) Cortical and subcortical afferent connections of the primate's temporal pole: A study of rhesus monkeys, squirrel monkeys, and marmosets. J. Comp. Neurol. *242:*425–458.

McGaugh, J.L., I.B. Introini-Collison, L. Cahill, M. Kim, and K.C. Liang (1992) Involvement of the amygdala in neuromodulatory influences on memory storage. In J.P. Aggleton (ed): The Amygdala: Neurobiological Aspects of Emotion, Memory, and Mental Dysfunction. New York: Wiley-Liss, pp. 431–451.

Meunier, M., J. Bachevalier, M. Mishkin, and E.A. Murray (1993) Effects of visual recognition of combined and separate ablations of the entorhinal and perirhinal cortex in rhesus monkeys. J. Neurosci. *13:*5418–5432.

Moran, M.A., E.J. Mufson, and M.-M. Mesulam (1987) Neural inputs into the temporopolar cortex of the rhesus monkey. J. Comp. Neurol. *256:*88–103.

Murray, E.A., E.A. Gaffan, and R.W. Flint, Jr. (1996) Anterior rhinal cortex and the amygdala: Dissociation of their contributions to memory and food preference in rhesus monkeys. Behav. Neurosci. *110:*30–42.

Myers, R.E., and C. Swett (1970) Social behavior deficits of free-ranging monkeys after anterior temporal cortex removal: A preliminary report. Brain Res. *18:*551–556.

Nakamura, K., K. Matsumoto, A. Mikami, and K. Kubota (1994) Visual response properties of single neurons in the temporal pole of behaving monkeys. J. Neurophysiol. *71:*1206–1221.

Pitkänen, A., and D.G. Amaral (1991) Demonstration of projections from the lateral nucleus to the basal nucleus of the amygdala: A PHA-L study in the monkey. Exp. Brain Res. *83:*465–470.

Porrino, L.J., Crane, A.M., and P.S. Goldman-Rakic (1981) Direct and indirect pathways from the amygdala to the frontal lobe in rhesus monkeys. J. Comp. Neurol. *198:*121–136.

Price, J.L., F.T. Russchen, and D.G. Amaral (1987) The limbic region. II. The amygdaloid complex. In A. Bjorkland, T. Hokfelt, and L. Swanson (eds): Handbook of Chemical Neuroanatomy. Amsterdam: Elsevier, pp. 279–381.

Rosvold, H.E., A.F. Mirsky, and K.H. Pribram (1954) Influence of amygdalectomy on social behavior in monkeys. J. Comp. Physiol. Psych. *47:*173–178.

Saunders, R.C., and D.L. Rosene (1988) A comparison of the efferents of the amygdala and the hippocampal formation in the rhesus monkey: I. Convergence in the entorhinal, prorhinal and perirhinal cortices. J. Comp. Neurol. *271:*153–184.

Saunders, R.C., D.L. Rosene, and G.W. Van Hoesen (1988) Comparison of the efferents of the amygdala and the hippocampal formation in the rhesus monkey: II. Reciprocal and non-reciprocal connections. J. Comp. Neurol. *271:*185–207.

Stefanacci, L., and D.G. Amaral (1993) Organization of cortical inputs to the lateral nucleus of the monkey amygdala. Soc. Neurosci. Abstr. *19:*441.

Suzuki, W.A., and D.G. Amaral (1994a) The perirhinal and parahippocampal cortices of the macaque monkey: Cortical afferents. J. Comp. Neurol. *350:*497–533.

Suzuki, W.A., and D.G. Amaral (1994b) Topographic organization of the reciprocal connections between the monkey entorhinal cortex and the perirhinal and parahippocampal cortices. J. Neurosci. *14:*1856–1877.

Suzuki, W.A., and D.G. Amaral (1996) The construction of straight line unfolded two-dimensional density maps of neuroanatomical projections in the monkey cerebral cortex. Neurosci. Protocols. *96:*1–19.

Suzuki, W.A., S. Zola-Morgan, L.R. Squire, and D.G. Amaral (1993) Lesions of the perirhinal and parahippocampal cortices in the monkey produce long-lasting memory impairment in the visual and tactual modalities. J. Neurosci. *13:*2430–2451.

Szabo, J., and W.M. Cowan (1984) A stereotaxic atlas of the brain of the cynomolgus monkey (*Macaca fascicularis*). J. Comp. Neurol. *222:*265–300.

Teuber, H.L. (1972) Unity and diversity of frontal lobe functions. Acta Neurobiol. Exp. *32:*615–656.

Tigges, J., M. Tigges, N.A. Cross, R.L. McBride, W.D. Letbetter, and S. Anschel (1982) Subcortical structures projecting to visual cortical areas in squirrel monkey. J. Comp. Neurol. *209:*29–40.

Turner, B.H., M. Mishkin, and M. Knapp (1980) Organization of the amygdalopetal projections from modality-specific cortical association areas in the monkey. J. Comp. Neurol. *191:*515–543.

Ungerleider, L.G., and M. Mishkin (1982) Two cortical visual systems. In D.J. Ingle, M.A. Goodale, and R.J.W. Mansfield (eds): Analysis of Visual Behavior. Cambridge, MA: MIT Press, pp. 549–598.

Van Essen, D.C., and J.H.R. Maunsell (1983) Hierarchical organization and the functional streams in the visual cortex. TINS *6:*370–375.

Van Hoesen, G.W. (1981) The differential distribution, diversity and sprouting of cortical projections to the amygdala in the rhesus monkey. In Y. Ben-Ari (ed): The Amygdaloid Complex. Elsevier/North-Holland Biomedical Press, pp. 77–90.

Van Hoesen, G.W., and D.N. Pandya (1975) Some connections of the entorhinal (area 28) and perirhinal (area 35) cortices of the rhesus monkey. I. Temporal lobe afferents. Brain Res. *95:*1–24.

Weiskrantz, L. (1956) Behavioral changes associated with ablation of the amygdaloid complex in monkeys. J. Comp. Physiol. Psych. *49:*381–391.

Whitlock, D.G., and W.J.H. Nauta (1956) Subcortical projections from the temporal neocortex in *Macaca mulatta.* J. Comp. Neurol. *106:*183–212.

Zola-Morgan, S., L.R. Squire, D.G. Amaral, and W.A. Suzuki (1989) Lesions of perirhinal and parahippocampal cortex that spare the amygdala and hippocampal formation produce severe memory impairment. J. Neurosci. *9:*4355–4370.

Zola-Morgan, S., L. Squire, P. Alvarez-Royo, and R.P. Clower (1991) Independence of memory functions and emotional behavior: Separate contributions of the hippocampal formation and the amygdala. Hippocampus *1:*207–220.